Development of Enhanced Cylindrical Specimen Thermal Conductivity Testing Procedure

by

Derek Morris

A Thesis Presented in Partial Fulfillment
of the Requirements for the Degree
Master of Science

Approved October 2011 by the
Graduate Supervisory Committee:

Kamil Kaloush, Chair
Barzin Mobasher
Patrick Phelan

ARIZONA STATE UNIVERSITY

December 2011

ABSTRACT

The current method of measuring thermal conductivity requires flat plates. For most common civil engineering materials, creating or extracting such samples is difficult. A prototype thermal conductivity experiment had been developed at Arizona State University (ASU) to test cylindrical specimens but proved difficult for repeated testing. In this study, enhancements to both testing methods were made. Additionally, test results of cylindrical testing were correlated with the results from identical materials tested by the Guarded Hot-Plate method, which uses flat plate specimens.

In validating the enhancements made to the Guarded Hot-Plate and Cylindrical Specimen methods, 23 tests were ran on five different materials. The percent difference shown for the Guarded Hot-Plate method was less than 1%. This gives strong evidence that the enhanced Guarded Hot-Plate apparatus in itself is now more accurate for measuring thermal conductivity.

The correlation between the thermal conductivity values of the Guarded Hot-Plate to those of the enhanced Cylindrical Specimen method was excellent. The conventional concrete mixture, due to much higher thermal conductivity values compared to the other mixtures, yielded a P-value of 0.600 which provided confidence in the performance of the enhanced Cylindrical Specimen Apparatus.

Several recommendations were made for the future implementation of both test methods. The work in this study fulfills the research community and industry desire for a more streamlined, cost effective, and inexpensive means to determine the thermal conductivity of various civil engineering materials.

To my wife and son, who were there for me

each step of the way.

And for my parents who showed me

how to walk in the first place.

ACKNOWLEDGMENTS

The author wishes to thank the National Center of Excellence (NCE) for SMART Innovations at Arizona State University for sponsoring this project and for provided an ideal setting to host both experiments. The NCE is supported by principle members such as BASF – The Chemical Company, which provided funds to advance testing methods in this research study.

Many, many thanks belong to Dr. Kamil Kaloush and Dr. Barzin Mobasher for the time, guidance, and encouragement they provided to this research project. Special thanks also go to Dr. Phelan for his input and guidance on this work, and Peter Goguen for his assistance in various laboratory troubleshooting activities.

TABLE OF CONTENTS

Page

CHAPTER Page

LIST OF TABLES

Table Page

LIST OF FIGURES

Figure Page

Figure Page

Chapter 1

INTRODUCTION

1.1 PROBLEM STATEMENT

With an ever-increasing interest in the environmental impact of material manufacturing and use, industries are investing in technologies that reduce the footprint of their product. In the application of civil engineering materials, thermal conductivity is becoming an important property to integrate into their construction process. Thermal conductivity is defined as the ability of a material to conduct heat. If, for example, a structure located in a hot climate consists of walls whose material is of low thermal conductivity, the inner temperature will resist changes in the exterior temperature, thus keeping it cooler indoors.

The current method of measuring thermal conductivity, according to the ASTM C 177-97 standard, labeled in this report as Guarded Hot-Plate, requires a flat plate of dimensions $2.54 \times 30 \times 30$ cm ($1 \times 12 \times 12$ in.). Fabrication of such samples is not difficult when materials are able to be molded or cut. But for most common civil engineering materials, such as conventional concrete, creating or extracting such samples is difficult. This ASTM code even discourages testing of these types of inhomogeneous materials, stating that specimens exhibiting appreciable in-homogeneities in the heat flux direction shall not be tested. The code continues that there are two potential problems in attempting to determine the heat flux through highly inhomogeneous specimens. The first relates to the interpretation and application of the resulting data. The second is the degradation in the performance of the apparatus. This method of determining thermal conductivity was generally intended for homogonous materials. In contrast, concrete possesses larger aggregates, thus making accurate results difficult to obtain.

A model of the Guarded Hot-Plate was designed and tested at the National Center for Excellence (NCE) for SMART Innovations at Arizona State University (ASU) to determine the thermal conductivity of various concrete samples. Yet, unforeseen difficulties and errors arose and repeated testing became excessively time consuming and cumbersome to perform. To utilize the common industry geometric shape of a cylinder having a 10.2 cm (4 in.) diameter and 17.8 cm (7 in.) height, a Cylindrical Specimen apparatus was also developed. Problems and time constraints also made this method difficult to implement into industry standards. In order to use this promising method of testing in industrial applications, time-consuming processes and extraneous assembly requirements need to be simplified or removed.

1.2 PURPOSE AND SCOPE OF STUDY

A prototype thermal conductivity experiment had been developed at ASU to test cylindrical specimens but proved difficult for repeated testing. Therefore, the cylindrical thermal conductivity concept was utilized to create a redesigned and enhanced apparatus that will more easily test cylindrical specimens. The apparatus was validated by confirming the thermal conductivity results of known calibration samples. Additionally, the results of cylindrical testing were correlated with the results from identical materials tested by the Guarded Hot-Plate method. This will fulfill the NCE and industry desire for a more streamlined, cost effective, and inexpensive means to determine the thermal conductivity of various civil engineering materials such as concrete mixtures.

1.3 OUTLINE OF REPORT

This report contains five chapters that will discuss the process of developing, testing, and analyzing the data for the new test methods. Chapter 2 includes a literature

review and introduces various current methods of testing for thermal conductivity. Chapter 3 describes the reasoning for the development of the modifications to the two methods and their respective testing procedures. Chapter 4 lists each type of material used. Chapter 5 provides the test results, including the correlations between the Guarded Hot-Plate and Cylindrical Specimen test methods. Chapter 6 includes the conclusions of the study and future recommendations.

Chapter 2

LITERATURE REVIEW

2.1 INTRODUCTION

With approximately 12 billion tons of raw materials going into the production of concrete each year, the concrete industry has become the largest consumer of resources in the world (Mehta 2002). Concrete makes its way to the urban environment in many forms, and whether it is used for building foundations, roadways, sidewalks, or structural exteriors, the type of concrete used greatly influences the heat transfer properties of its surface. Those types of concrete that have a greater tendency to store heat become warm during the daytime and delay the transferring of that heat into the atmosphere until several hours after sunset. This large amount of stored heat contributes to what is known as the Urban Heat Island (UHI) effect that occurs in urban environments, as shown in Figure 1.

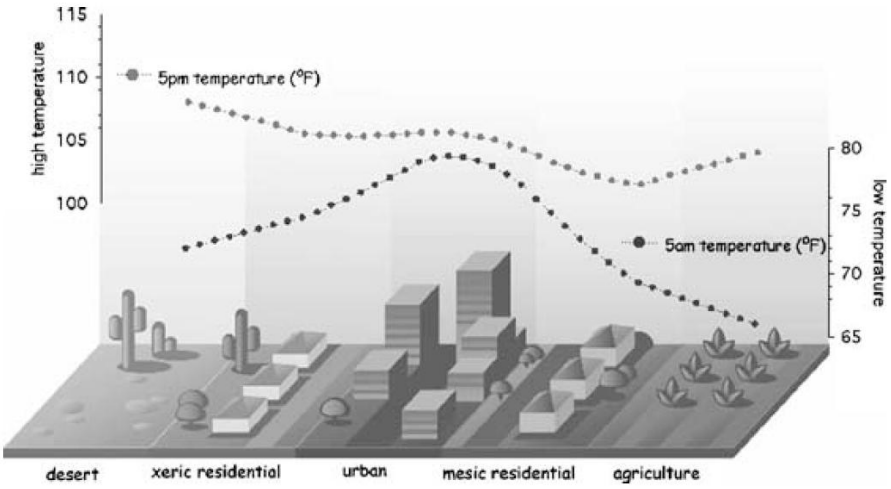

Figure 1: UHI Effect on Temperature in Desert vs. Urban Climate (Golden 2004)

In contrast, materials low in thermal conductivity mitigate the release of heat back into the atmosphere, minimizing temperature peaks and producing desirable affects. Therefore, industries are expressing more interest in how they can better utilize the heat transfer characteristics of materials. A wall system manufactured by Meccano de México has had success in producing cast-in-place fully integrated molds for multi-component wall casting. As shown in Figure 2, the entire exterior is layered with a fiber reinforced thermal layer to improve the thermal efficiency.

Figure 2: Meccano de México Fiber Reinforced Thermal Layer Exterior (Zhu et al. 2010)

This includes the prefabricated thermal layer complemented by a cast in place concrete on the inner wall. Not only does this layered wall system contribute to the comfort of those within the home, but it also reduces the UHI affect since less heat is stored in this urban fabric. As can be seen from many additional applications, properly utilizing the heat transfer properties of materials can greatly enhance the benefits to both the producer and consumer.

2.2 HEAT TRANSFER

The simple concept of heat describes that energy available for transferring from one system to another when a temperature difference exists. It is the rate and method by which heat is transferred that is the primary concern of this study. Just as the voltage

difference is the driving force for electric current and flow, and pressure difference is the driving force for fluid flow, temperature difference is the driving force behind heat transfer (Çengel 2003). In the following sections, several terms will be defined that pertain to heat transfer. Then an introduction of the methods of heat transfer will be given. With the many methods that have been developed to measure the thermal conductivity in past years, several related studies will be presented. The last study, the ASU Cylindrical Specimen thermal conductivity test method, will be described in detail as it is the basis for the development of this study's enhanced Cylindrical Specimen apparatus design and procedure.

DEFINITIONS

Thermal Conductivity, k – This coefficient is represented as *k* commonly in watts per meter times Kelvin (W/m-K) or BTU/h-ft-^{o}F and is defined as the rate of heat transfer through a unit thickness of a material per unit area for each unit temperature difference. Thermal energy generally takes place by means of conduction, which occurs when energetic particles transfer their energy to less energetic particles. Conductivity will be described in detail in following sections. For conduction, a one-dimensional analysis of thermal conductivity, *k* (in W/m-K), employs Fourier's law, as given by the following equation and conceptually represented by the temperature gradient in Figure 3.

$$Q_{cond} = -kA\frac{dT}{dx} \tag{1}$$

Where: Q_{cond} = heat flux or power applied over a given area, W/m^2

A = surface area subject to heat flux, m^2

$\frac{dT}{dx}$ = temperature gradient through material in the x direction

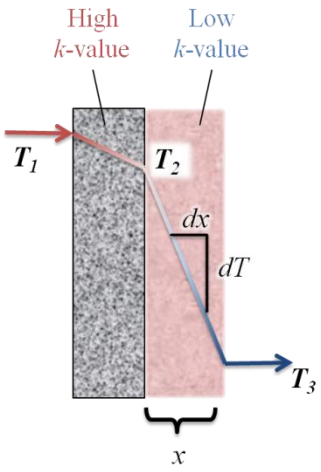

Figure 3: Heat Transfer through Two Materials

The thermal conductivity, *k*, measures the effectiveness that heat is transferred through a given material thickness *dx* ($x_1 - x_2$). A material that effectively transfers heat, such as copper, is known as a conductor. A conductor would have a very high thermal conductivity and the *dT* ($T_1 - T_2$) in Equation 1 would be very small as a result. An insulator, such as foam, would have a very low thermal conductivity and thus a large *dT*. Since air serves as a very effective insulator, any form of air gap will be properly addressed in this study.

Thermal conductivity is affected by several factors, such as the density, porosity, and moisture content of the material. The impact of each on thermal conductivity will be given in their respective definition sections. Concerning concrete specifically, thermal conductivity is dependent on the type of mix, the aggregates it contains, and amount of compaction. A list of the thermal conductivity values of common materials is shown below.

Table 1: Thermal Conductivity of Common Materials ([1] Young 1992; [2] Hukseflux 2011)

Material	Thermal Conductivity, W/m-K
Acrylic Glass, Plexiglas	0.17 - 0.2
Air	0.024[1] - 0.025[2]
Aluminium, pure	205[1] - 237[2]
Conventional Concrete	0.8[1] - 1.28[2]
Copper, pure	385[1][2]
Fiberglass	0.045[2]
Glass	0.8[1] - 0.93[2]
Gold, pure	314[1]
Lead, pure	34.7[1]
Water	0.6[1]

Thermal Resistance, R – The resistivity of a material determines its resistance to heat transfer for a temperature difference across the thickness. It is given as the reciprocal of the thermal conductivity, or 1/*k*, in units of m-K/W. A small thickness of a material with a high thermal conductivity will yield a low resistance to heat transfer. For this reason, thin copper plates are used as the material for the framing of the Guarded Hot-Plate apparatus.

Density, ρ – This property is a measure of the mass per volume of a material and is represented by the Greek symbol, ρ.

$$\rho = \frac{m}{V} \tag{2}$$

Where: ρ = density, kg/m^3 (lb$_{mass}$/ft^3)

m = mass, kg (lb$_{mass}$)

V = volume, m^3 (ft^3)

A material with a high density tends to have a higher thermal conductivity, while the opposite is true of lower density materials.

Moisture Content, M% – This represents the percentage by weight of water contained in a material and is determined by the following equation.

$$M\% = \frac{N-D}{D} \tag{3}$$

Where: *M%* = moisture content, %

N = original mass of sample, kg (lb)

D = dry mass of sample, kg (lb)

The effect that moisture content has on the thermal conductivity of a material is due to the higher thermal conductivity of water than air, 0.6 to 0.024 W/m-K, respectively (Young 1992). Since water fills the pores that air previously inhabited, the overall ability for the material to transfer energy has been increased and the thermal conductivity will be significantly more than the dried sample. For this reason, the detailed procedures in Appendix C and D give instructions to dry each specimen before testing to minimize the transient behavior caused by moisture content within the material.

Specific Heat, c_p – The specific heat of a material is defined as the amount of energy required to raise the temperature of one cubic centimeter of water by degree Celsius, and has units of J/kg-K or Btu/lb_{mass}-^{o}F. This thermal property can also be determined by knowing the thermal conductivity, *k*, thermal diffusivity, α, and the density, ρ, of the specimen.

$$c_p = \frac{k}{\alpha\rho} \tag{4}$$

Thermal Diffusivity, α – By utilizing the specific heat, c_p , and thermal conductivity, the thermal diffusivity can be determined. This represents how fast heat transfers through a material and can be found by solving Equation 4 for thermal diffusivity, α.

$$\alpha = \frac{k}{\rho c_p} \quad (5)$$

As an additional component of this equation, the heat capacity, ρc_p, represents how much energy a material stores per unit volume. By combining the definitions of the inputs to Equation 5, the thermal diffusivity can be seen as the ratio of the heat conducted through the material to the heat stored per unit volume (Çengel 2003). According to this definition, a material with a large thermal diffusivity will propagate heat faster into the medium.

MODES OF HEAT TRANSFER

Heat transfer that involves any type of energy transfer can be categorized into three different modes: conduction, convection, and radiation. These are further explained in the following sections.

Conduction **–** Conduction can occur within solid material, liquids, or gases whenever a temperature gradient exists. This is restricted to heat that flows through the matter itself, in contrast to having the energy transfer through motion of the matter. When occurring in solids, conduction is due to the combination of the vibrations of atoms in a lattice, known as lattice vibration. In solids, heat conduction occurs from lattice vibration waves and from the free flow of electrons. Lattice vibration occurs when the atoms that are faster than those in colder regions transfer their energy to their neighboring colder atoms in the lattice, which then begin to vibrate faster. This process continues and results in heat transfer from the hotter to cold side of the specimen, and can be shown in Figure 4.

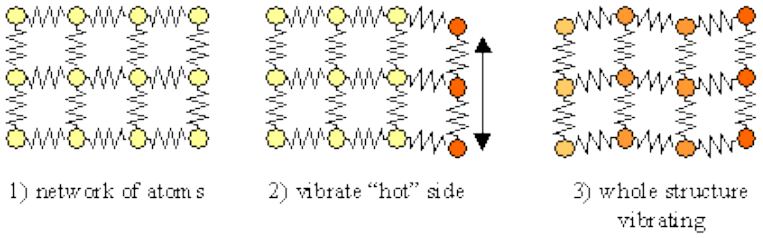

Figure 4: Conduction Energy Transfer by Means of Lattice Vibration (Tada 2002)

A faster form of heat transfer is due to electron flow, which is a component of pure metals. In this case, electrons freely move between the lattice structure of the solid. The total conductivity of a material is a combination of both the lattice vibration and electron flow.

Convection – This type of heat transfer occurs in a liquid or gas. When convection is due only to temperature differences, it is referred to as natural convection. Forced convection is created by the use of a fan or pump. In both cases, the hotter fluid or gas is actively replaced by the flow of cooler fluid or gas, and the heat transfer rate is increased. The faster the fluid motion, the faster will be the rate of heat transfer by means of convection. A simple example of forced convection may be a fan used on a ceiling to move air and cool the warm bodies that are in the room. Newton's law of cooling expresses the convection heat transfer rate, Q_{conv} (in W/[unit time]), to be proportional to the temperature difference of the two mediums, as shown in Equation 6.

$$Q_{conv} = hA_s(T_s - T_\infty) \tag{6}$$

Where: h = convection heat transfer coefficient, W/m^2-^{o}C

A_s = surface area of heat transfer, m^2

T_s = surface temperature of material, ^{o}C

T_∞ = temperature of fluid sufficiently far from surface, ^{o}C

Understanding the definition of convection, one may also consider it as "conduction with fluid motion."

Radiation **–** Another method of heat transfer is represented by earth's greatest heat source, sunlight, in the form of thermal radiation. Radiation occurs by electromagnetic waves, or light, that are emitted by any matter with a temperature greater than absolute zero (-273 ^{o}C) and that are then absorbed by another matter. When discussing radiation in terms of heat transfer, the primary concern is thermal radiation, which does not include forms of electromagnetic radiation such as x-rays, microwaves, or gamma rays. In contrast to conduction and convection, radiation requires no medium to transfer its energy. Yet this method transfers heat faster than the other two methods: at the speed of light. An introduction to the mechanics of thermal radiation can be offered by Stefan-Boltzmann's law, which defines the maximum rate of radiation emitted from a surface at a given temperature, $\dot{Q}_{emit,max}$.

$$\dot{Q}_{emit,max} = \sigma A_s T_s^4 \tag{7}$$

Where: σ = Stefan-Boltzmann constant, 5.67E-08 W/m^2-K^4

T_s = absolute temperature of the surface, K

A_s = surface area, m^2

Any combination of all three modes of heat transfer may play part in warming an object. For example, radiation may be significant relative to conduction or natural convection, but plays little role in forced convection, and is, therefore, disregarded in those cases. Thermal radiation in the form of sunlight may contact a window, transferring through the glass medium by means of conduction and then warming the room inside by means of convection. As seen by this example, all three methods may need to be considered in heat transfer studies.

2.3 MEASURING METHODS

There are many methods used to determine thermal conductivity, each necessitating specimens of particular material and geometry. Over time, convenience of circumstance and limits of knowledge have been the largest factors in determining what type of apparatus and method result. Although many additional methods exist, several of the common methods will be described in the following sections. Concluding these methods will be the recent development by the National Center for Excellence for SMART Innovations at Arizona State University to use cylindrical specimens.

Guarded-Hot-Plate Apparatus **–** This method is governed by ASTM C 177-03, *Standard Test Method for Steady-State Heat Flux Measurements and Thermal Transmission Properties by Means of the Guarded-Hot-Plate*. This setup is used to determine the thermal conductivity of homogonous materials, such as insulations, and the specimens are formed with slab geometries. This method has been used in determining the thermal conductivity of both concrete and asphalt (Tan et al. 1992).

The apparatus consists of vertical layers, with symmetry above and below the middle axis. The center section consists of a metered area known as the guarded hot plate, which is thermally isolated by a primary guard on all sides. Above and below this center section are placed the test specimens, followed by isothermal cold surface assemblies. The entire apparatus is then wrapped along the horizontal circumference by insulation. An illustration of the location of and heat flow, *Q*, among these main components is shown in Figure 5.

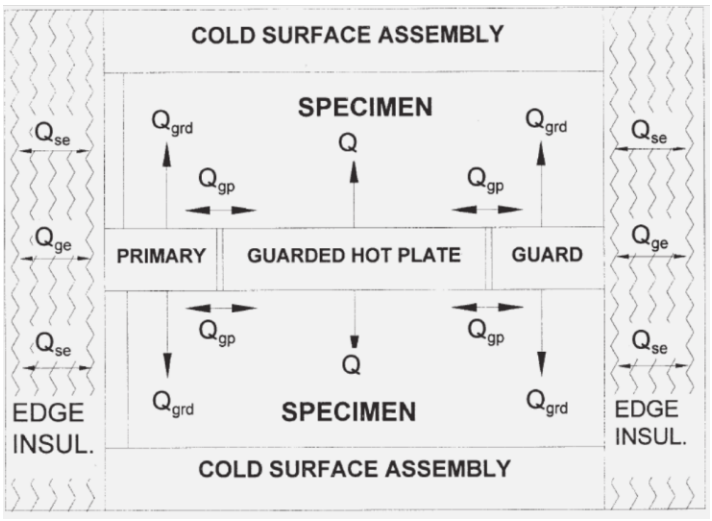

Figure 5: ASTM C 177 Idealized Arrangement of the Guarded Hot-Plate Apparatus

The metered section containing the main heater is sandwiched between surface plates of high thermal conductivity (generally copper or aluminum). The primary guard consists of guard heaters similarly sandwiched between the guard surface plates (also of copper). The use of a distributed electrical resistance heating element is recommended since it disperses the energy uniformly across the metered and primary guard sections. As depicted in Figure 5 by the symbol Q_{gp}, the energy transfer across the air gap between the primary guard and metered section serves to thermally isolate the two sections and assist in the metered section maintaining its accuracy of measurement. This gap is not required but assists in minimizing edge loss effects. The temperature difference between the metered and primary guard sections should not exceed 0.2 K. By providing a steady-state, one dimensional heat flux from the heaters through the two specimens, half the heat is transferred to each. For this reason, the two specimens should be selected with thicknesses, areas, and densities as identical as possible for that material.

Once the energy transfers through the specimens, the cold surface assemblies act as isothermal heat sinks that remove the energy from the specimens. The temperature of

the top and bottom surface of each specimen is utilized to determine thermal conductivity. Therefore, thermocouples are used to record the temperature at several points on each side of the specimen and in both the metered and primary guard sections, though corners and edges of each section should be avoided.

An additional factor to be considered is the specimen maximum thickness, which is one-third the maximum linear dimension of the metered section. Also, specimens containing large inhomogeneous materials should be avoided, since the resulting data may be unrepresentative of another cross section of the specimen.

Once the apparatus is prepared with samples, the temperature of the primary guard heaters and metered section heater are maintained to within 0.2 K of each other and the temperatures are recorded until a steady-state thermal condition is established. The power supplied by the metered section heater, Q_{heater}, is calculated using the voltage (in volts), V, and the current (in amperes), I, in the following equation.

$$Q_{heater} = V \times I \tag{8}$$

The thermal conductivity, k, is then obtained by using the ratio of metered power, Q_{heater}, to the metered section area, A, and specimen thickness, x, as follows.

$$k = \frac{Q_{heater}(x)}{A(T_1 - T_2)} \tag{9}$$

The last consideration for Equation 9 is to take the symmetry into account. Since there are two specimens that share the power, the final equation used in testing is:

$$k = \frac{Q_{heater}(x)}{2A(T_1 - T_2)} \tag{10}$$

This equation provides the thermal conductivity for each specimen using the Guarded Hot-Plate apparatus.

University of New Brunswick k-alpha Tester – As designed and developed by the University of New Brunswick (UNB), the UNB *k*-alpha tester attempted to address the problem of accounting for edge losses. As introduced by Luca and Mrawira (2002) and further described in their later report (2005), a critical challenge they wished to solve was the seeming inability for other apparatus to achieve a one-dimensional steady state heat flow for specimens due to their thin slab requirement. By the new methodology of UNB, two identical specimens of dimensions $100 \times 100 \times 20$ mm are placed on both sides of a main heater and sandwiched between two heat sinks, as shown in Figure 6.

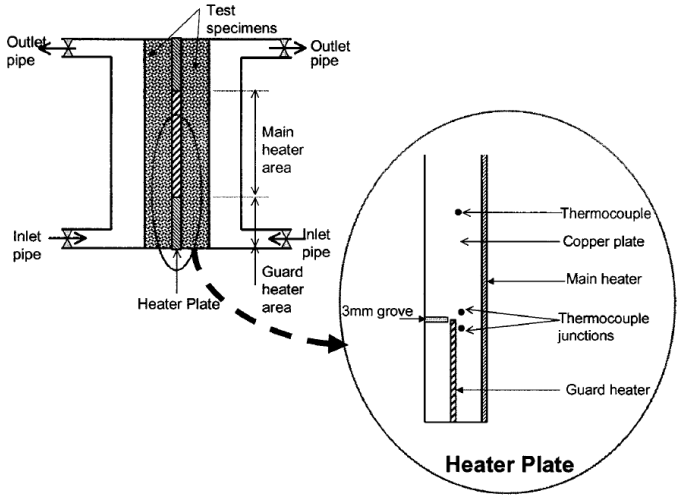

Figure 6: Schematic of UNB *k*-alpha Tester (Luca and D. Mrawira 2005)

The specimen required careful cutting from a 15 cm (5.9 in.) diameter compacted briquettes. Their procedure also requires a maximum 1.27 cm (0.5 in.) thickness for the aggregates. Once the specimen, heater, and cooling plates are fit together, the assembly is brought to a uniform initial temperature before beginning the test. This initial temperature value is maintained on the heat sink side of the apparatus over the duration of the experiment by adjusting the DC power supply of the main heater and primary guard heater until a thermal equilibrium is reached. Using high-resolution DC voltage and

current meters, including thermocouples for temperature measurement, the power as given in Equation 8 and thermal conductivity can be determined. This method also utilizes Equation 10 to determine the thermal conductivity. In conclusion, though very similar to the Guarded Hot-Plate apparatus, the sample size represents the largest difference since these smaller samples may be obtained from cylinder cores, which are more available in industrial uses than are the flat slab specimens used for the Guarded Hot-Plate.

Transient Plane Source Method **–** The theory of the Transient Plane Source (TPS) method is introduced by Al-Ajlan (2006). One of the most beneficial reasons for using TPS is its ability to produce accurate measurements for numerous materials having a large range of thermal conductivity values. It also produces results in a very short time, anywhere from 10 seconds to 10 minutes. There are many types of transient techniques, all generally comprised of a signal that is sent into the sample to create heat, after which the response is measured. For this reason, these techniques require only a short time to obtain the measurements. The TPS technique has similar roots as other transient methods, being first established as the Gustafsson probe or the hot disk (Gustafsson 1991).

The TPS sensor consists of a strip wound into a number of concentric circles made into double spirals. This strip is coated with a thin polymer, Kapton in many cases. The concentric circles allow for the current to continue from one end to the other while the polymer coating provides the option to test electrically conducting materials. Yet, Al-Ajlan primarily tested insulation-type specimens in his report. Gustafsson provides a diagram of the experiment in Figure 7, which shows the sensor placed between two material specimens.

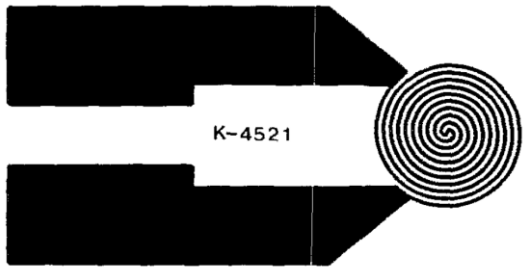

Figure 7: "Hot Disk" Design for Transient Plane Source Method

It is the thermal contact resistance between the sensor and the sample that induces a temperature difference. The increase of this resistance measured over time is given as the following function:

$$R(t) = R_0[1 + \varphi\{\Delta T_i + \Delta T_{ave}(\tau)\}] \quad (11)$$

Where R_0 is the resistance of the disk prior to being heated, φ is the temperature coefficient of the resistivity, ΔT_i is the temperature difference over the thin insulating layers covering the two sides of the hot disk sensor, and $\Delta T_{ave}(\tau)$ is the temperature increase on the opposite side of the specimen's insulating layer that is facing the hot disk sensor. By combining the inputs of Equation 11 and the theory representing the time-temperature increase of Equation 12 below, the thermal conductivity is determined.

$$\Delta T_{ave}(\tau) = \left[P_0/\left(\pi^{3/2} ak\right)\right] D(\tau) \quad (12)$$

In this equation, P_0 is the power output from the sensor, a represents the surface area of the circular disk, k is the thermal conductivity, and $D(\tau)$ represents a time-dependent function, further explained in the report of Al-Ajlan (2006).

2.4 ASU CYLINDRICAL SPECIMEN METHOD

The concept of the Urban Heat Island (UHI) has been of great interest to Arizona State University. At the National Center for Excellence (NCE), an additional procedure for measuring the thermal conductivity was developed to more effectively address the UHI issue. This method utilizes the geometry of a cylindrical specimen as these are the most commonly available specimens in the pavement industry. The cylindrical shape permits aggregate sizes in the concrete that are larger than the 2.54 cm (1 in.) thickness given in the Guarded Hot-Plate method. It is also much easier to fabricate or extract from in-service projects than the $2.54 \times 30 \times 30$ cm ($1 \times 12 \times 12$ in.) slab required for Guarded Hot-Plate specimens. Industries may utilize these cylinders for mechanical testing, volumetric property verifications, and quality control operations (Witczak et al. 2002), which typically have a diameter of 10 cm (4 in.) and a height of 15 to 20 cm (6 to 8 in.).

By utilizing this common geometry, the need for additional samples to be created for thermal properties testing would be greatly reduced or even eliminated. Therefore, an apparatus was designed and built at the NCE to accommodate this cylindrical standard. The results from this study produced thermal conductivity values within acceptable levels of sufficient accuracy to provide confidence when using the method.

THEORETICAL ANALYSIS

The methodology and procedure is discussed by Carlson (2010). By utilizing explanations provided by Çengel (2003), the study introduces the topic of heat conduction in cylinders with Fourier's law, previously given in Equation 1. The heat source is applied to the center of the cylinder by the use of a cartridge heater. The

cylindrical form replaces *dx* with *dr*, where *r* is the radius of the cylinder, as given in the adjusted Equation 13 for heat transfer, $\dot{Q}_{cond,cyl}$.

$$\dot{Q}_{cond,cyl} = -kA\frac{dT}{dr} \tag{13}$$

The variables are separated and the equation is integrated from the inner to outer radius of the cylinder, r_1 *to* r_2, respectively. By setting the area as $A = 2\pi rL$, the thermal resistance of the cylinder, R_{cyl}, is represented as follows:

$$R_{cyl} = \frac{\ln(r_2/r_1)}{2\pi Lk} \tag{14}$$

By using the length of the cylinder, *L*, and the inner- and outer-radius temperature readings, T_1 and T_2, the heat transfer equation across a cylinder wall is rearranged.

$$\dot{Q}_{cond,cyl} = 2\pi Lk\frac{T_1 - T_2}{\ln(r_2/r_1)} \tag{15}$$

Ideally, this radial heat transfer would occur on a cylinder of infinite length, yet with a length of only 15.2 to 20.3 cm (6 to 8 in.), edge heat losses were inherent in solving for thermal conductivity, shown as $\dot{Q}_{loss}$ in the insulation portion of Figure 8.

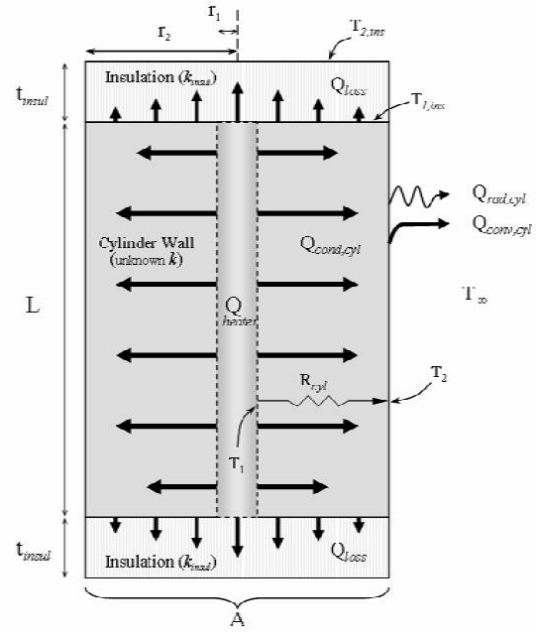

Figure 8: Theoretical Heat Transfer in Cylindrical Specimen (J. D. Carlson et al. 2010)

Therefore, an attempt was made to account for the heat losses on the top and bottom surface of the cylinder. These losses were accounted for by setting the following equality:

$$\dot{Q}_{cond,cyl} = \dot{Q}_{heater} - \dot{Q}_{loss} \tag{16}$$

The axial losses were estimated using the thermal conductivity of the insulation layer, k_{insul}, the insulation layer thickness, t_{insul}, the circular area of contact, A, and the temperatures at the bottom and top of the insulation, $T_{1,insul}$ and $T_{2,insul}$, respectively.

$$\dot{Q}_{loss} = k_{insul} A \frac{T_{1,insul} - T_{2,insul}}{t_{insul}} \tag{17}$$

By solving Equation 14 for k, and utilizing Equation 16, the following is found:

$$k = \frac{\dot{Q}_{cond,cyl} \ln (r_2/r_1)}{2\pi L (T_1 - T_2)} \tag{18}$$

Lastly, by combining Equations 8, 16, and 17, the final Equation as used by the NCE for their basis for their test design is determined.

$$k = \frac{[(VI) - \dot{Q}_{loss}] \ln (r_2/r_1)}{2\pi L (T_1 - T_2)} \tag{19}$$

EXPERIMENTAL DESIGN

The sample is prepared by coring the center of the cylinder with a 1.12 cm (0.437 in.) hole, careful to maintain symmetry through height of the cylinder to ensure uniform radial heat distribution from the heater. The heat source was a 55 Ohm cartridge heater that extended the height of the specimen and was connected to a programmable DC power supply. By designing the cartridge heater to be 0.318 cm (0.125 in.) smaller than the cored diameter of the hole, room was left for the insertion of the inner-wall thermocouples. An inner-wall insert was added to make the location of the inner-wall thermocouples more accurate, being one-quarter the length from the top and one-quarter

the length from the bottom. The location of the inner- and outer- wall thermocouples, along with the inner-wall insert, are shown in Figure 9.

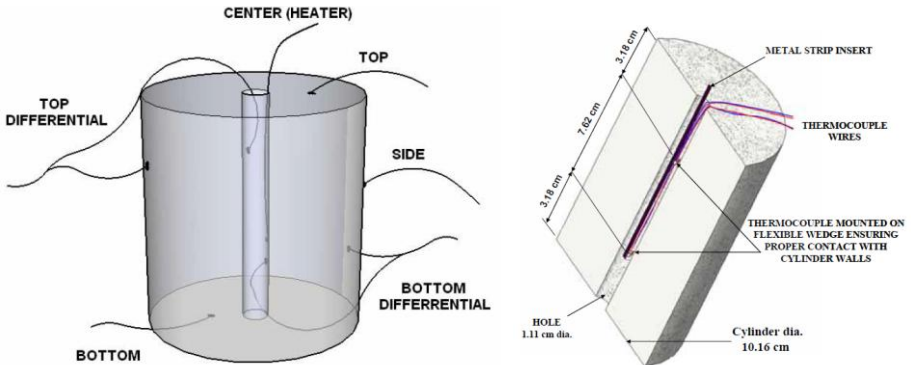

Figure 9: Location of Absolute and Differential Thermocouples on Cylinder (left) and Revised Inner-Wall Thermocouple Insert (right) (J. D. Carlson et al. 2010)

Yet the slight difference between the diameter of the cartridge heater and the inner radius of the cylinder created an air gap. This air gap prevented uniform heat transfer to the cylinder. Therefore, a high thermal conductivity paste was used to fill the gap and permit efficient heat transfer.

Thick insulation was placed above and below the sample after placing the thermocouples and cartridge heater. The apparatus was held together using several clamps and placed in an environmental chamber, as shown in Figure 10.

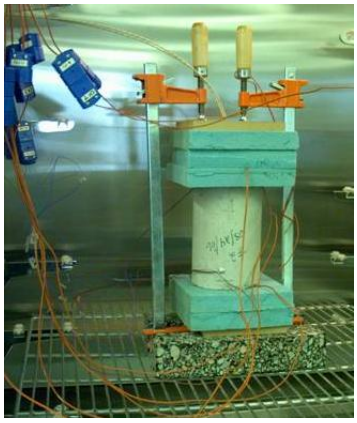

Figure 10: Clamped Cylindrical Specimen Apparatus in Environmental Chamber

The environmental chamber is maintained at 20^{o}C. The thermocouples are connected to a data acquisition system for temperature recording. Eight runs were performed for each type of mixture: Ultra High Molecular Weight Polyethylene (UHMWP), Hot Mix Asphalt (HMA), and Portland Cement Concrete (PCC). The NCE determined percent uncertainty values compared with stated literature values to be 5.1%, 2.6%, and 2.8% for UHMWPE, HMA, and PCC, respectively. The close correlation of these results, including additional uncertainty analyses, indicated an acceptable level of accuracy and repeatability for their test method.

Chapter 3

EXPERIMENTAL DESIGN

3.1 MODIFICATIONS AND DESIGN

In reviewing the Guarded Hot-Plate and Cylindrical Specimen thermal conductivity testing methods performed by the NCE at ASU, a greater efficiency and effectiveness was sought. The thesis work performed by Chong (2006) for the Guarded Hot-Plate and the study performed by Carlson (2010) for his Cylindrical Specimen apparatus gave indication of improvements that would simplify and improve the testing experience of each. Suggestions were taken into account and considered for modifications that would provide the greatest impact. These modifications are described below, including the respective design and testing procedures for each method.

3.2 GUARDED HOT-PLATE APPARATUS

MODIFICATIONS TO NEW APPARATUS

In 2006, the National Center for Excellence at Arizona State University developed an apparatus per the American Society for Testing and Materials (ASTM) guideline C 177-04, entitled "Standard Test Method for Steady-State Heat Flux Measurements and Thermal Transmission Properties by means of the Guarded Hot-Plate Apparatus" (ASTM, 2004). This method determines the thermal conductivity of homogonous specimens with dimensions $2.54 \times 30 \times 30$ cm ($1 \times 12 \times 12$ in.) and allows for adjustments to be made to the described apparatus design, granted they conform to the general requirements of the procedure. In a summary of the performance of this initial apparatus, the four greatest difficulties were mentioned concerning the condensation created by the chilled-water supply, the thermocouples, the uneven

specimen planes, and the bulkiness of the apparatus (Chong 2006). Each of these will be discussed including their respective solutions as implemented into the modified Guarded Hot-Plate apparatus.

Condensation **-** The ASU design utilized the available chilled water supply located in the testing laboratory and included copper tubing as shown in Figure 11. This satisfied the ASTM requirement for isothermal heat sinks to remove the energy generated by the heating units.

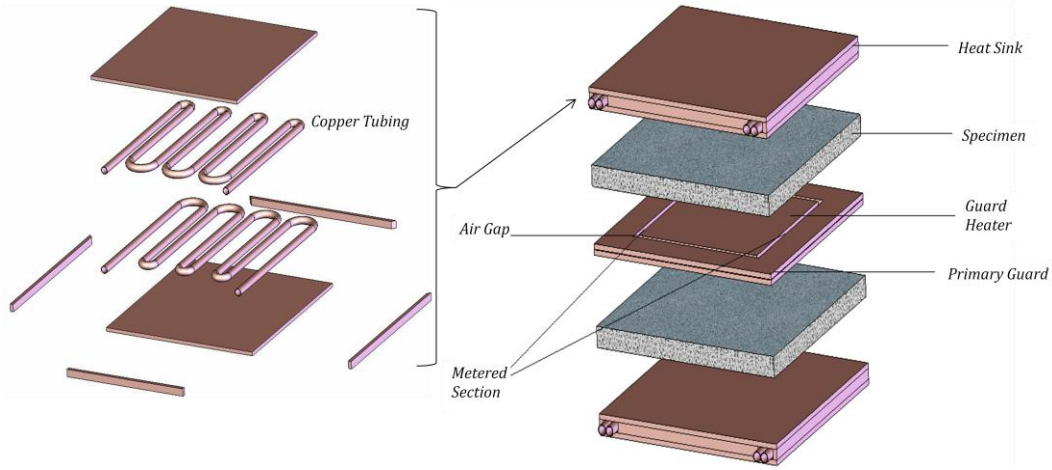

Figure 11: Initial Guarded-Hot-Plate Design at ASU (Kaloush, Carlson, Golden, & Phelan, 2008)

As testing continued, several difficulties arose that made the dismantling process for repeated testing time-consuming and cumbersome. Additionally, the chilled water produced excessive amounts of condensation on the piping and surrounding plates that migrated onto the concrete samples. Since the ASTM method warned that the thermal transmission properties may be affected by moisture conditions, an alternative was sought to remove the need of chilled water as the heat sink. To resolve this issue, a three-by-three array of aluminum heat sinks replaced the top and bottom copper tubing. Each heat

sink was attached to the copper plate using a thermal adhesive. To complete the replacement of the chilled-water supply, cooling fans were attached to the middle row of heat sinks for each side as shown in Figure 12. This removed the previous concerns of affecting the thermal conductivity measurements due to additional moisture on the specimens and that of running electrical equipment adjacent the wet apparatus.

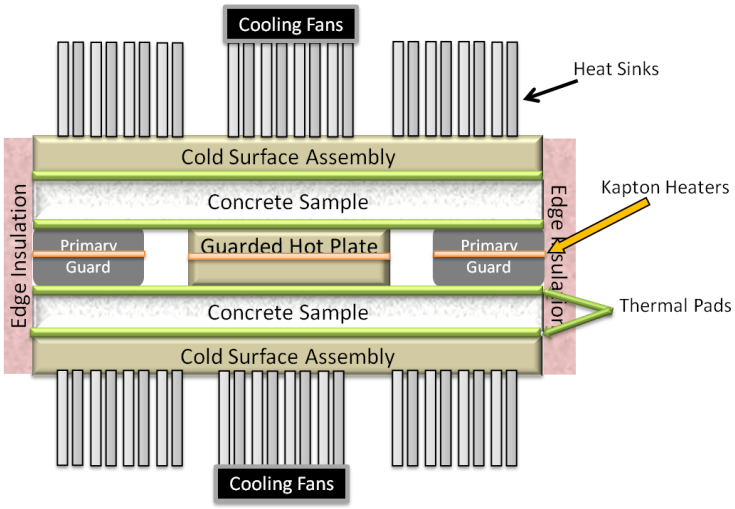

Figure 12: Modified Guarded-Hot-Plate Apparatus

Thermocouples & Uneven Plane **-** The initial design also caused many thermocouples to tear under the heavy copper plates as samples were adjusted and replaced. Small, 30-gauge T-Type thermocouples were placed on the upper- and lower-side of each specimen since there was very little flexibility between layers to install temperature sensors. These were attached using thermally conductive Kapton tape over the surface area. Though the thin-diameter thermocouples minimized the air gap created by their presence, that characteristic contributed to their fragility and likelihood of breaking during test runs.

Additionally, possible error due to air gaps was introduced due to the inherent difficulty of making $2.54 \times 30 \times 30$ cm ($1 \times 12 \times 12$ in.) concrete samples sufficiently smooth to provide direct contact with the copper plates. Concrete samples often

possessed small irregularities, and removing such by sanding or grinding would jeopardize the integrity of the specimen. To resolve this problem, the thermocouples for each layer were attached to a thermally conductive silicone sponge rubber pad which was placed between the upper- and lower-side of the top and bottom samples using Kapton tape. This is according to section 7.2.2.2 of the ASTM Guarded Hot-Plate method to mount a compressible thin sheet between the plates to improve the uniformity of the thermal contact.

By also using clamps on all four corners of the apparatus, the segments fit snug to each other, and the silicone pads better conformed to the irregularities in the sample. This permitted thermocouples to be permanently placed over the surface of the silicone pads as suggested in Section 6.7 of the ASTM Guarded Hot-Plate method. The pads resolved both issues of breaking thermocouples and of an uneven specimen surface. They also greatly increased the speed and consistency of repeated tests since the pads could be easily removed and adjusted without having to reattach the thermocouples to each sample.

Bulkiness – During experimentation using the previous apparatus, a mechanical lifting instrument was suggested to assist with the heavy load of copper plates and concrete specimens during assembly and thermocouple adjustment (Chong 2006). The chilled-water supply tubes further complicated the process by making it difficult to rest the plates on their sides. To resolve the issue of bulkiness, a support structure was designed to levitate the entire apparatus. This permitted for air-flow from the added cooling fans on the top and bottom. As shown in Figure 13, the support structure included three vertical beams used to rest the upper cold surface assembly and sample while either changing out samples or making adjustments to the various layers of the assembly. The completed

apparatus resting on the support structure is shown in Figures 13 and 14 (note that the outer insulation is not in place in Figure 14).

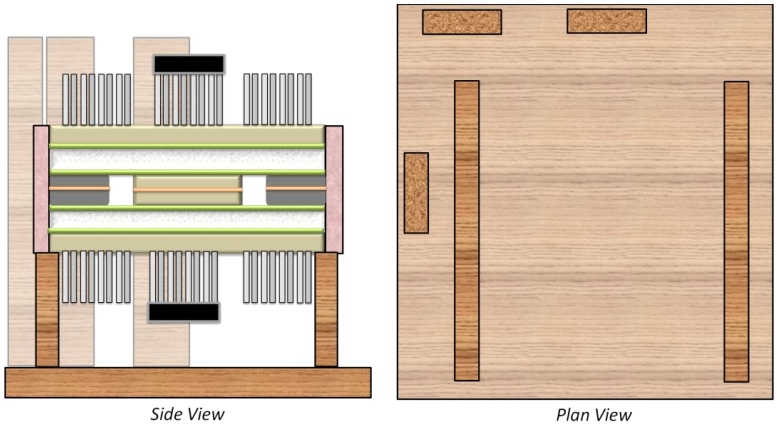

Figure 13: Side and Plan View of Modified Guarded-Hot-Plate Support Structure

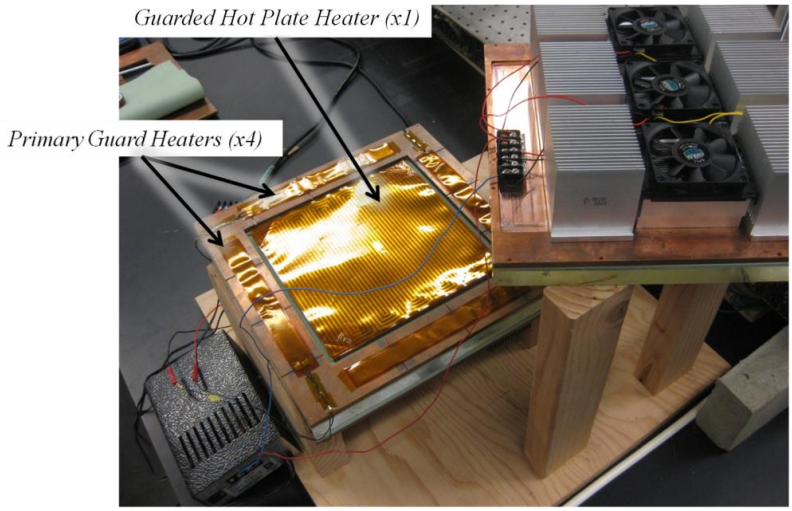

Figure 14: Modified Apparatus with Plexiglas Sample (Showing Kapton Heaters)

As a result of the modifications made, the aforementioned difficulties of using the initial apparatus were eliminated. The updated apparatus tested samples more efficiently and required only a few minutes to replace and begin testing the next specimen after the apparatus cooled off to ambient temperatures.

DESIGN

In modifying the initial Guarded Hot-Plate apparatus, many details remained unchanged while other fundamental changes were made. Therefore, a detailed graphic is provided in Appendix A. Using Figure 12, this discussion will begin at the top layer and proceed through the layers to the center of the symmetric apparatus.

Cooling Fans & Heat Sinks – Three 12-Volt cooling fans attached to aluminum heat sinks, commonly used for processor cooling on a PC motherboard, lined the center of 3 rows of heat sinks. These were oriented so that all heat sink blades were parallel, thus maximizing removal of heat by the air flow draw created by the center row of cooling fans. To maximize heat transfer to the heat sinks from the copper plate cold surface assembly, the thermal adhesive Arctic Silver™ was used. This paste has a thermal conductivity greater than 7.5 W/m-K (Arctic Silver 2011) which, at a thickness of less than 0.03 cm (0.01 in.), negligibly affects the heat transfer of the system .

Copper Plate Assemblies – The top and bottom layers consist of a flat, pure copper sheet to which the cooling fans are attached. The center copper plates that house the main and primary guard heaters are sized according to the ASTM specifications and are shown in Figure 15. The 0.5 cm (0.2 in.) wide isothermal region between the primary guard and center section provides an air gap that isolates the metered center section and prevents lateral heat flow from escaping.

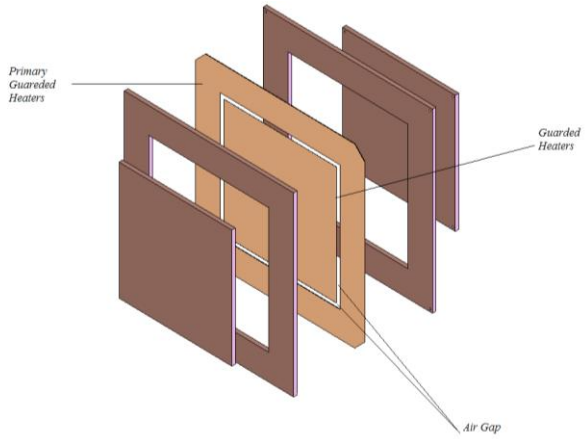

Figure 15: Layered View of Main and Primary Guard Heaters Housed in Center Copper Plates (K. E. Kaloush et al. 2008)

Silicone Sponge Rubber Pads – Four pads total were used on the top and bottom of each specimen. These pads were provided by Therma Cool® and had a 0.318 cm (0.125 in.) thickness and 30 × 30 cm (12 × 12 in.) surface. When fully assembled, the apparatus is under a slight compression and the manufactures provide a table to compensate for the thermal conductivity of the pad for respective compression percentages, as shown below for two thicknesses of pads. The impact to the heat transfer across the additional thickness of the pads will be accounted for in the Calculations Section 5.2.

Table 2: Thermal Conductivity of Silicone Pads (Saint-Gobain Performance Plastics 2010)

	Thermal Conductivity, W/m-K	
Compression, %	**1/8" Pad**	**1/16" Pad**
10	0.36	0.36
30	0.52	0.46
50	0.86	0.57

The pads are layered with the concrete sample so that the side with the thermocouples makes direct contact with the sample. Four thermocouples are located in the center over the guard heater (highlighted box) and two thermocouples are placed over the area of the outer primary guard as shown in Figure 16. On this figure, each "x" marks a thermocouple location, with 24 thermocouples in total.

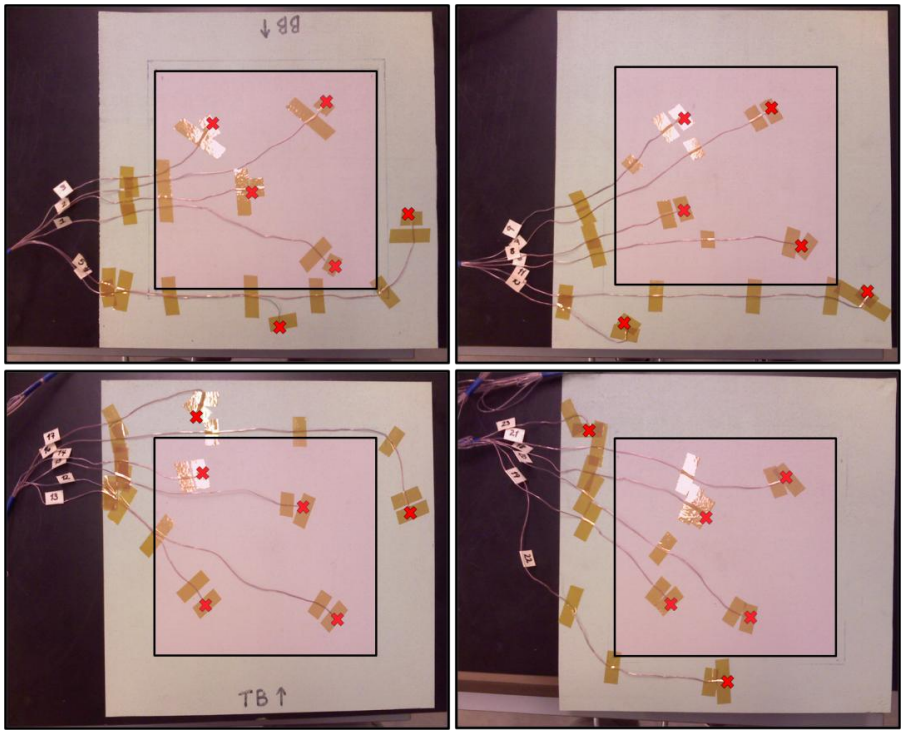

Figure 16: Four Silicone Pads with Thermocouple Locations

Thermocouples and Data Acquisition **–** The 24 thermocouples, as shown on Figure 16, are 30-gauge, Omega T-Type thermocouples. The temperature acquisition end of each thermocouple is stripped of its plastic cover and the constantan and copper wires are soldered together at the very tip to create an absolute thermocouple configuration. In this case, due to the thin gauge of the wire, the last 0.64 cm (0.25 in.) of the ends was tightly twisted together instead, thus assuring a solid contact between the two metals.

Temperature data is collected using a National Instruments Data Acquisition (DAQ) system, chassis SCXI 1000 with Terminal Port 1303. A virtual instrument (VI) is created using LabView to properly store and label the data for analysis. The thermocouples were calibrated with the DAQ, per the stated calibration procedure of National Instruments, using a Haake™ water bath at 10, 30, 50, 70, and 90°C, as shown in Figure 17.

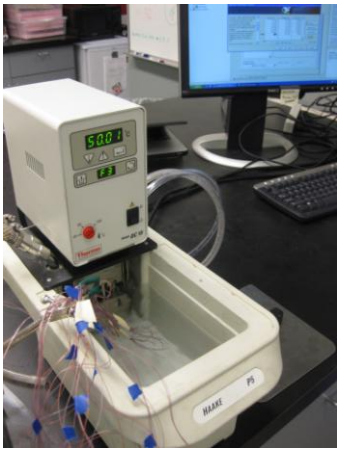

Figure 17: Calibration of Thermocouples Using Controlled Water Bath (lid removed)

Measuring Voltage, Current, and Power – A digital multimeter is utilized to measure the voltage of both the main heater and primary guard heaters over the course of each testing period. This is done by placing it in parallel with each respective circuit. The current must be measured by placing the digital multimeter in series with each circuit. Both values are then substituted into Equation 8 to determine the power provided by the heater, $\dot{Q}_{heater}$. Both variacs are initially adjusted to provide similar temperature outputs within 0.2 K between the metered section surface plate (warmed by the main heater) and the primary guard surface plate (warmed by the primary guard heaters) (ASTM C 177-97 2003).

Heaters and Variac – As shown on Figure 14, there are four primary guard heaters and one main heater, the guarded hot plate heater. The main heater is an Omega Kapton Flexible Heater (#KH-110/5) that has a 0.042025 m^2 (8 × 8 in.) area.

Figure 18: Omega Kapton Flexible Heater Used in the Metered Section (K. E. Kaloush et al. 2008)

The main heater is connected to a variable transformer (variac) to allow for voltage adjustments to be made. The four primary guard heaters are 2.54 × 20.32 cm (1 × 8 in.) strips. The concept for these heaters is to have an etched continuous circuit protected by the thermally conductive Kapton layer that holds it in place. At a thickness of 0.025 cm (0.01 in.), they create a minimal air gap when fitted between the two copper plates. These heaters are each connected to a separate variac in parallel circuit, allowing the voltage to the primary guards to be independently adjusted from that of the main heater.

Edge Insulation **–** Around the outer circumference of the assembled apparatus, a 2.54 cm (1 in.) thick Styrofoam insulation sheet was strapped snugly around the unit. This generic foam has an approximate thermal resistance of 0.03 W/m-k. The edge insulation serves as secondary guarding to restrict heat losses from the outer edge of the primary guard.

TESTING PROCEDURE

A full, step-by-step testing procedure is provided in Appendix C. The non-dry weight of each sample is recorded and the samples are heated in an oven at 80^{o}C for 48 hours to remove moisture. Any water content in the specimens can affect the results by increasing the measured thermal conductivity. Therefore, it will be recorded for later comparison. The moisture percentage is then calculated as described in Equation 3. During testing, the primary guard heaters prevent heat loss from the main heater (metered section). Therefore, the variac supplying power to the primary guard heater was initially calibrated before testing to maintain temperatures within 2% of the main heater temperature value.

Each layer of the apparatus is placed as shown in Figure 13 using the upper support structure stand as needed for the upper half of the apparatus. The thermocouples on the top and bottom silicone pads are faced toward the sample. The main and primary guard heaters are placed between the copper plates, and the top layers are put in place. The edge insulation is strapped in place to be snug around the apparatus. On each corner is a clamp used to compress the apparatus layers to fit snugly. Excess pressure is avoided in order to prevent bowing of the cold surface assemblies and, thus, breaking the bond of the thermal adhesive to the heat sinks.

Once the apparatus is in place, caution is taken to properly route the cooling fans, two variacs, DAQ, and computer to avoid overloading any circuits. The DAQ and LabView are first turned on to collect data followed by the heaters and fans. The specimens are allowed to heat up until the ASTM steady-state temperature requirement is met, which requires an increment of temperature difference to be less than 0.1% between data readings.

The data is then copied into a template developed to perform a data reduction process through MatLab and Excel which assists in quick analysis of the results. The data is reduced by a factor of four, n = 4, and the thermocouples on each layer are averaged together to yield one temperature measurement per layer. This significantly reduces the amount of data and calculates and plots the thermal conductivity, as given in Equation 10, versus time.

3.3 CYLINDRICAL SPECIMEN APPARATUS

MODIFICATIONS TO NEW APPARATUS

In 2006, the National Center of Excellence at Arizona State University designed an apparatus to test the thermal conductivity of the 10.2 cm (4 in.) diameter, 17.8 cm (7 in.) tall cylindrical specimens. Several mixes and specimens were successfully tested, yet as repeated testing continued, troublesome aspects of the design and setup became more apparent. These were recorded by Carlson (2010) and the following sections discuss how they were resolved.

Coring Diameter – In contrast to the flexible Kapton heaters on the Guarded Hot-Plate apparatus, cylindrical specimens were heated using a 55 Ohm cartridge heater (FIREROD^{TM}, Part No. G6A83 – Watlow Electric Manufacturing Company, St. Louis, Missouri, USA) having a 15.2 cm (6 in.) length and a 0.953 cm (0.375 in.) diameter. One concern was to ensure symmetry in the hole while coring the specimen for the heater. Though drill presses were used and drilling began on center, the exit points of some holes were off-center since the small-diameter coring bit curved when hitting aggregate.

Alternate core bit diameters were researched and a 2.54 cm (1 in.) diameter bit was found to meet the design needs for the new apparatus. This coring bit is more

common and less expensive than specialty diameter bits. Accuracy during drilling increased and additional benefits were gained that will be discussed in future sections. With the increased size for the coring bit came a need for an increased diameter for the cartridge heater. Omega cartridge heaters with a diameter of 1.91 cm (0.75 in.) replaced the smaller heaters. This adjustment led to more symmetric and straighter center holes, thus increasing the accuracy of the testing and of the resulting data. A visual comparison between the sizes of the old and new cartridge heaters and the typical accuracy of the exit points for the coring bits is shown in Figure 19.

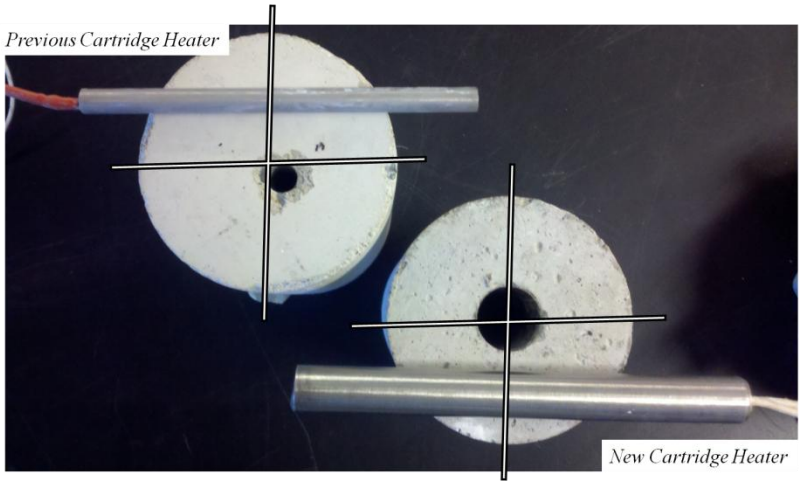

Figure 19: Exit Points of Previous and New (0.75 in.) Coring Bit Diameters and Respective Cartridge Heaters

Silicone Sponge Rubber Pad – For the previous design, the 0.953 cm (0.375 in.) hole-diameter was designed to be 0.318 cm (0.125 in.) larger than the heater diameter to permit thermocouples to fit inside. To fill in this gap, the hole and heater were coated with a thermally conductive paste, manufactured by Omega Inc. The paste was used up quickly and made for difficult cleaning between samples. The thermocouples were meant to measure the inner surface of the specimen wall, but one could not be sure whether or not they were in contact with the heater instead, thus giving the incorrect temperature.

As utilized for the modified guarded hot-plate apparatus, silicone sponge rubber pads proved very functional for the cylindrical design. A 0.318 cm (0.125 in.) thick pad was sized to fit between the specimen and 1.91 cm (0.75 in.) diameter cartridge heater, as shown in Figure 20.

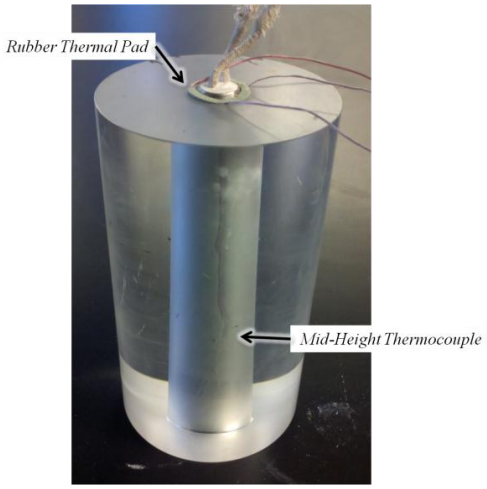

Figure 20: Side View of Acrylite® Specimen, Rubber Pad and Thermocouple Shown

During setup, the three thermocouples allocated for measuring inside the center hole are slid through past the bottom surface, allowing them to be pulled back up into the apparatus to their designated locations along the height of the inner specimen once the heater and pad are in place. This eliminates the need for the paste to fill the gap and allows for accurate placement of the thermocouples. Cleanup time between specimens is greatly reduced and the speed between runs is increased. With this more airtight fit of the pad and cartridge heater, caution must be taken when inserting and removing each item.

Support Structure – After laboriously placing the thermocouples in the center hole of the initial apparatus, the tips of the thermocouple intended for measuring the external cylindrical temperature were secured to the cylinder using a highly conductive (10 W/m-^{o}C) silver adhesive (J. D. Carlson et al. 2010). A solid contact between the thermocouple

and measuring surface is important to obtaining accurate measurements. Unfortunately, the strong bond of silver adhesive made removing and replacing the thermocouples from specimen to specimen quite difficult.

An alternative to the adhesive must provide solid contact and consistent measurements. Thus, a support structure was fabricated to house several V-shaped bars containing thermocouple slots, as shown in Figure 21, designed for quick release and reapplication of the needed contact pressure after the next specimen is inserted. Detailed diagrams are available in Appendix B.

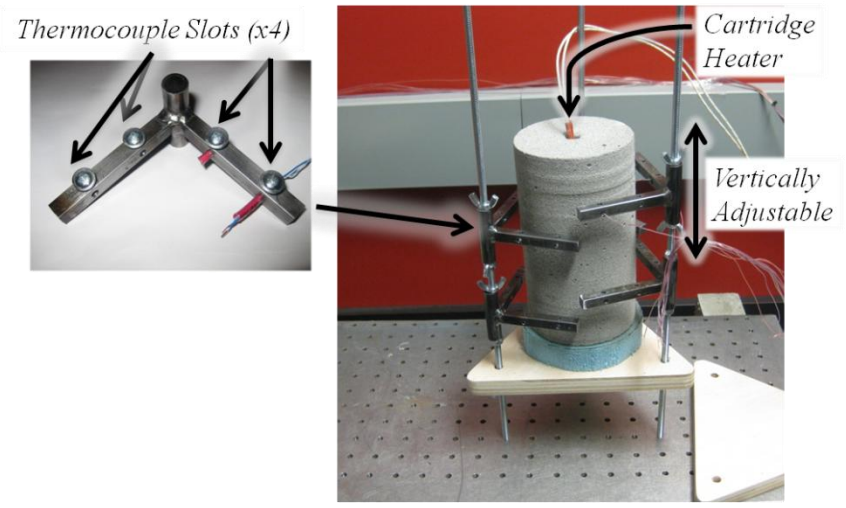

Figure 21: Location of Thermocouple Slots on V-shaped Bar

The cylindrical specimen is placed on top the triangular base board and 2.54 cm (1 in.) thick foam insulation, with another layer of foam and board above the specimen. A slit is cut into the upper triangular board to allow the cartridge heater and center-hole thermocouple wires to be easily moved in and out between testing. The entire apparatus is then lightly compressed by tightening wing nuts placed above and below the apparatus on each dowel rod.

Testing of Multiple Specimens – Once assembled, the entire initial cylindrical specimen apparatus was placed in a 1.5 cubic meter environmental chamber that served as the heat sink for the experimental system by maintaining the air temperature around the specimen at 20^{o}C. Several observations were made after repeated tests using the environmental chamber setup. One comment related to the inconvenience of setting up the apparatus, needed thermocouples, and supply wires for the cartridge heater. Once testing began, making small adjustments or even visually inspecting the backside of the apparatus was difficult due to the restricted working area as shown in Figure 10.

An additional comment concerned the time-consuming process for testing multiple specimens, since the time needed for preparing and then testing one sample required nearly a full day. A means for multiple testing was included in the enhanced Cylindrical Specimen apparatus design, as shown in Figure 22, allowing for three specimens to be simultaneously tested.

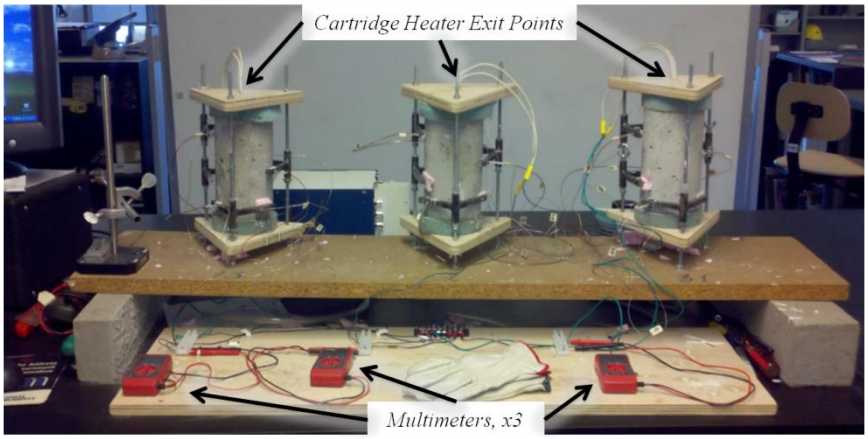

Figure 22: Enhanced Cylindrical Specimen Apparatus with Multiple Sample Setup

By conducting the experiment in a lab room with a stable climate of 22^{o}C, the initial need for an environmental chamber was overcome. Utilizing the same National Instruments Data Acquisition (DAQ) system as with the Guarded Hot-Plate experiment,

the available thirty measurement channels were split to serve nine thermocouples for each of the three specimens. The remaining thermocouples were available to measure the ambient temperature. Additionally, one variac supplied power to the three cartridge heaters through a parallel circuit. Due to the modified open-air setup, one could now observe, measure, and make any necessary adjustments to the specimens from any angle before and during testing.

DESIGN

Although an introduction to various aspects of the enhanced design was given throughout the Modifications section, this section presents every component of the apparatus. Refer to Appendix B for a detailed diagram.

Support Structure – By screwing the three metal dowel rods for each apparatus into the 1.2 m (4 ft.) long base, the apparatus for all three specimens can be placed adjacent each other and help keep the setup organized. This apparatus base is elevated 15 cm (6 in.) above the circuitry and multimeter board. The triangular board of each apparatus has three holes near each corner slightly larger than the 0.635 cm (0.25 in.) dowel rod. By using a top and bottom triangular board, one can apply the appropriate pressure to the entire apparatus using wing nuts on each hole of the board. There are four V-shaped bars on each apparatus and each of the three dowel rod has two, one, and one V-shaped bar, respectively, adjusted at random heights for a variety of placement of the thermocouples along the height of the specimens.

Thermocouples Placement – There are seven thermocouples located on each apparatus, as shown on Figure 23, comprising 21 thermocouples in all. Additional channels of the

DAQ remain for thermocouples to measure radial temperature of the cylinder on the top and bottom and to measure ambient temperature of the lab room.

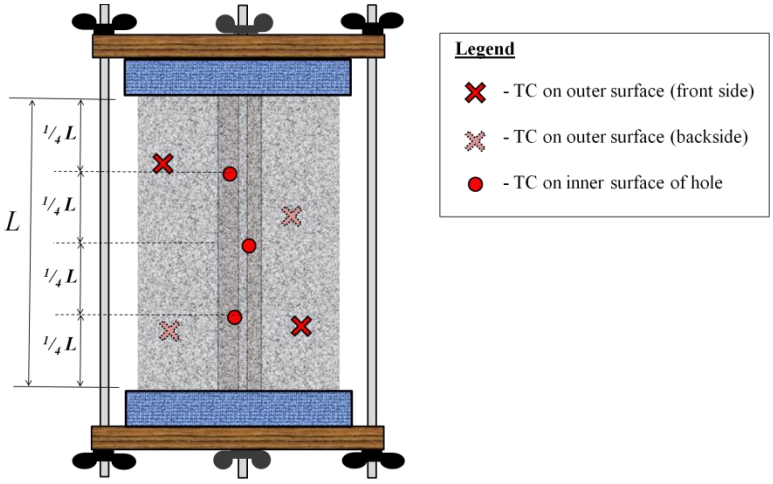

Figure 23: Approximate Locations of Thermocouples on Cylindrical Specimen Apparatus (side view)

Similar to the Guarded Hot-Plate thermocouples, 30-gauge, Omega T-Type thermocouples are used. Due to the thin gauge of the wire, the last 0.635 cm (0.25 in.) of the ends was tightly twisted together, instead of using a soldering method.

Four holes are in each V-shaped bar to offer variety for thermocouple placement along the horizontal circumference of the specimen. A vertical hole is threaded from the top to the center to give grip for a small screw that will hold the thermocouple rod in place. This is shown in Figure 21. Once the thermocouples are tightened into place, a small amount of Omega Thermal Paste is used to surround the contact point of the thermocouple junction tip with the surface of the concrete as shown in Figure 24.

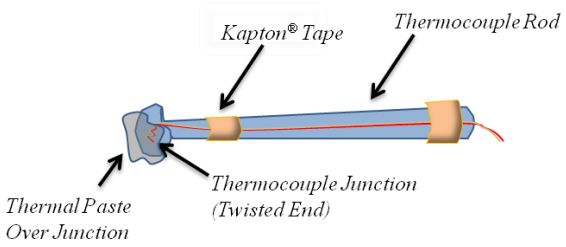

Figure 24: Thermocouple Rod with Thermal Paste

When placing the exterior thermocouples, the top and bottom 2.54 cm (1 in.) are avoided to minimize the consequence of edge loss on the temperature reading.

Insulation – To mitigate heat loss from the top and bottom surfaces of the specimen, 2.54 cm (1 in.) thick sheets of insulation are placed on top and bottom of the sample, having a thermal conductivity of 0.02 W/m-K. Both are sized to extend beyond the edge of the cylinder by at least 1.27 cm (0.5 in.). The top insulation has a small hole cut in the middle including a thin slit from the middle to the circumference that is just large enough to permit sliding the heater and thermocouple wires through when assembling and disassembling the apparatus. An appropriately sized insulation piece is then placed snugly in the slit after sliding the wires through to further minimize heat loss from the top surface. This process is shown in Figure 25 below.

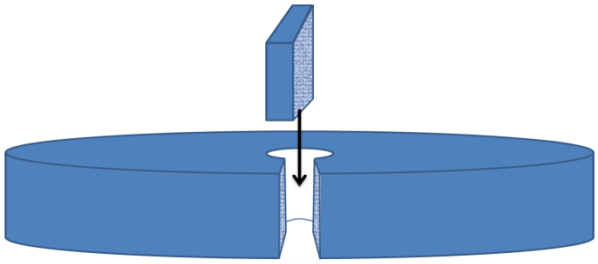

Figure 25: Foam Insulation with insertion piece

Data measurement - Temperature data is collected using a National Instruments Data Acquisition (DAQ) system, chassis SCXI 1000 with Terminal Port 1303. Figure 26 shows the DAQ including the thermocouple grouping for the cylindrical experiment.

Figure 26: National Instruments Data Acquisition System with Thermocouples

A virtual instrument (VI) is created using LabView to properly store and label the data for analysis. The thermocouples had been calibrated with the DAQ using a Haake™ water bath as similarly stated for the Guarded Hot-Plate Apparatus in Section 3.2.

TESTING PROCEDURE

A full step-by-step version of the procedure is located in Appendix D, and a plan view of the testing area layout for both experiments is shown in Figure 27 below. A variac capable of supplying at least ten amperes is set up to provide parallel power to each of the three apparatus setups. The board beneath the support structure is used to connect circuitry for the power. By using strip terminal connectors, a multimeter can be inserted in series and parallel to measure current and voltage, respectively.

Once dimensions and weight of cylinders are recorded, the samples are heated in an oven at 80^{o}C for 48 hours and the weight is again measured to calculate moisture content as described in the detailed procedure. They are then allowed to cool for two hours before testing.

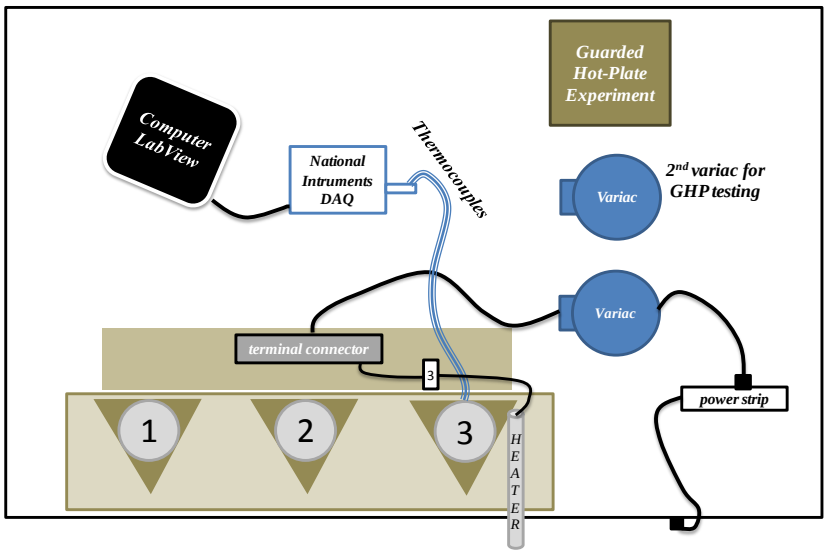

Figure 27: Testing Area for Both Experiments (Showing Setup Only to Third Cylinder Apparatus)

The three thermocouples used for the center hole of the cylinder are slid through slightly past the bottom of the hole. The thermal pad is placed in the center hole, using a smooth-tipped rod to remove any pad overlap if needed. The center thermocouples are then pulled up into the appropriate vertical positions as shown on Figure 23, and an example from a side view can be seen in Figure 20.

The cartridge heater is then pushed in place using a back-and-forth, rotating motion. The cylinder is placed in the apparatus atop the bottom triangular board and insulation piece. By utilizing the slits in the top insulation piece and triangular board, the wires from the cartridge heater and the thermocouples are pulled away from the top of the apparatus. The top triangular board is slightly and evenly compressed using the wing nuts for each of the three dowel rods once the cylinder is centered between the three dowel rods.

The outer thermocouples are placed using the appropriate locations on the V-shaped bars. For each thermocouple, a vertical screw (having a blunted end to prevent

piercing the thermocouple) is used to keep the thermocouple rod in place, and a small spacer is put between the specimen and V-shaped bar on the alternate end. Hence, the pivot at the dowel rod is the fulcrum to maintain contact with the thermocouple tip and specimen. Lastly, a spot of the Omega highly conductive paste is placed at the contact of the thermocouple and specimen to insulate this connection as shown in Figure 24.

The LabView software is initiated once all thermocouples are properly connected to the DAQ, power is supplied to the cartridge heaters, and measurement devices are in place to read current and voltage. The variac is then turned on and readings continue until a steady-state temperature is obtained.

Chapter 4

MIXTURE TYPES

4.1 DESCRIPTION OF MIXTURES

In order to validate the enhanced testing method of the Cylindrical Specimen apparatus, two calibration samples were tested using both methods, Acrylite® GP and Hardibacker® Backerboard. Additionally, samples included Aerated Fiber Reinforced Concrete (AFRC), Autoclaved Aerated Concrete (AAC), and a conventional Portland cement concrete sample. The sample dimensions and additional characteristics are provided in Appendix E.

Acrylite®GP – Two 2.54 cm (1 in.) thick, and 30 × 30 cm (12 × 12 in.) cross-section sheets of Acrylite® GP (commonly known as Plexiglas) were obtained from Piper Plastics of Chandler, AZ.

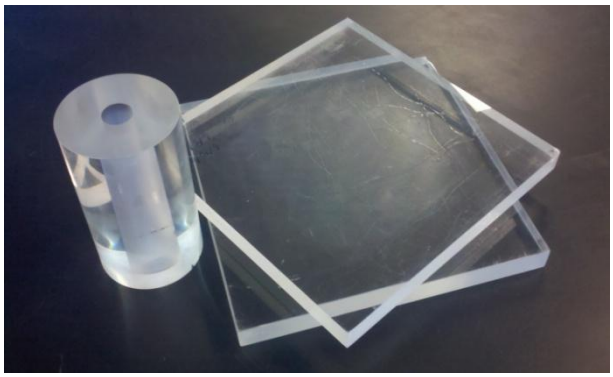

Figure 28: Acrylic Cylindrical and Flat-Plate Samples

These samples were used as a main calibration between the Guarded Hot-Plate and Cylindrical Specimen methods due to their homogeneity and consistency in reproduction,

i.e. obtained in same manner whether in cylindrical or plate form. The clear acrylic sheets are cell-cast and have a large variety of uses, from paneling to signs. As provided by TAPS Plastics, the supplier to Piper Plastics, Acrylite® GP has a stated thermal conductivity of 0.19 W/m-K. Also, as shown in Table 1, typical acrylic glass has a thermal conductivity from 0.17 to 0.20 W/m-K.

Hardibacker® Backerboard – As another calibration means for the Guarded Hot-Plate (though not for the Cylindrical Specimen apparatus), Hardibacker® Ceramic Tile Backerboard was used. It is a single-faced, cellulose fiber-reinforced cement building board and is commonly intended for interior walls and floors, including shower and bath areas. According to the ES Legacy Report, NER 405, the provided thermal conductivity is 2.30 BTU/hr-ft^2-^{o}F, or 0.33 W/m-K. The Backerboard was only able to be used to verify the accuracy of the Guarded Hot-Plate apparatus, since it could not provide accurate results if layered into a cylindrical form.

Aerated Fiber Reinforced Concrete (AFRC) - Aerated Concrete is a material having comparably low thermal conductivity and heat capacity. It is lightweight and noncombustible, and is a cement based material that is manufactured from a combination of Portland cement, fly ash or other sources of silica, quick lime, gypsum, water, and aluminum powder or paste. The air pores in aerated concrete are usually 0.1 to 1 mm in diameter, as shown in following figure, and the most common technique of creating them is by adding aluminum powder at about 0.2% to 0.5% by weight of cement. This is visible in Figure 29, which shows a 5.08×5.08 cm (2×2 in.) cross section of AFRC.

Figure 29: Cross Section of a 2 × 2 in. AFRC sample (Bonakdar and Mobasher 2010)

The mixture expands to about twice its volume as a highly porous structure is created. Approximately 80% of the volume of the hardened material is made up of pores, including 50% being air-pores and 30% being micro-pores (Holt and Raivio 2005). AFRC is classified based on its range of dry density, 400 to 800 kg/m^3 (25 to 50 lb/ft^3), and its range of compressive strength, 2 to 6 MPa (290 to 870 psi) (ASTM C 1386-07 2007). Although AFRC has a low thermal conductivity due partly to its low density, its lightweight quality permits it to be appropriate for 1-2 story buildings, since it also serves as a good sound insulator.

An additional pair of samples for testing was made to assist in confirming initial results and will be distinguished as AFRC_1 and AFRC_2, although the final data will be simply labeled AFRC. Due to the larger variation in data for the first two tests ran for this particular mixture, two additional tests were added. Duplicate samples were cut from blocks of the same mixture to run the additional tests.

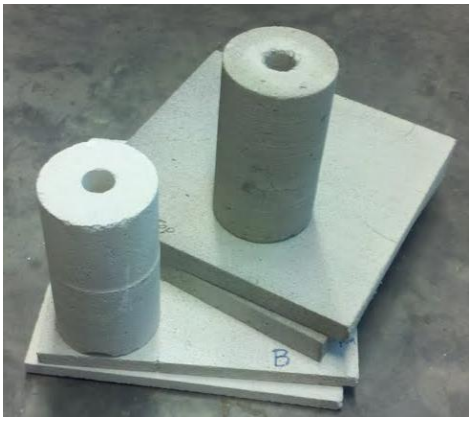

Figure 30: AAC Samples (Bottom Left) and AFRC Samples (Top Right)

Autoclave Aerated Concrete (AAC) – Autoclave Aerated Concrete has similar characteristics as AFRC, but contains no fiber reinforcement. The mixture contains a smaller amount of aluminum powder, 0.05% to 0.08% by volume, than AFRC. The aeration process also produces similar types of pore structures as that of AFRC. The report ASTM C 1386 – 07 introduces three strength classes, which are identical to those of the AFRC description.

After mixing the AAC, the method of autoclaving concrete involves placing the blocks into autoclave chambers to undergo a steam pressure hardening process, where quartz sand reacts with calcium hydroxide to form calcium silica hydrate. This accelerates the strength gain though the end strength will still be much less than that of conventional concrete. The result is a very lightweight concrete, advantageously used to provide structure, insulation, fire and mold resistance.

Conventional Concrete (FHWA) – A standard conventional Portland cement concrete mixture was prepared with the assistance of the Federal Highway Administration (FHWA), Office of Pavement Technology Program, Mobile Concrete Laboratory. Flat plates and cylindrical concrete specimens were sent by FHWA to ASU; these concrete

samples were obtained from a highway project in Indiana, and will thus be labeled FHWA. These samples were not pervious concretes and had almost a completely smooth outer surface, and this minimizes the likelihood of accidentally placing the thermocouples on an air gap. Unlike all other samples tested, these specimens contained coarser aggregates, and thus are inhomogeneous. Although this is not recommended by the ASTM C 177 – 97 for flat slab specimens, as quoted in Section 1.1 of this report, they were utilized as an additional comparison between the two testing methods. Since both the flat plate and cylindrical samples were poured and not cored, no cross sections of aggregates were visible. Otherwise, the placement of thermocouples would have been appropriately considered for direct contact with any inhomogeneous material having a different thermal conductivity.

It is noteworthy to mention that one purpose of the enhanced Cylindrical Specimen Apparatus is to determine whether or not accurate, repeated results for heterogeneous mixes can be obtained. This includes use by the industry which generally tests mixes of higher thermal conductivity, thus the addition of the FHWA samples. It is not the purpose of this study to report on the affects of different characteristics of the material, such as density and aggregate content, but simply to assure the mix is consistent between the two apparatus.

Chapter 5

TEST RESULTS AND ANALYSIS

5.1 TEST RESULTS

The final results comprised data thermal conductivity values from 23 tests, 11 using the Guarded Hot-Plate method and 12 from the Cylindrical Specimen method. Since the purpose of this study is to confirm the validity of the Cylindrical Specimen apparatus, the number of tests performed on each type of mixture varies according to its importance in literature values. This will help make the correlation between the two methods more robust. Additionally, the Hardibacker® Backerboard samples could not be effectively fabricated into a cylindrical form, as mentioned previously.

Samples were tested in random order on each respective apparatus and, for the Guarded Hot-Plate apparatus, the top and bottom samples were switched if repeatedly tested. These actions prevent time-based trends or errors to have an effect on the final data.

After performing the multiple tests, the data was collected and the temperature gradient ($T_1 - T_2$) across each specimen thickness was determined. Occasionally, a thermocouple was afterward determined to have greatly differing results than the other similarly grouped thermocouples. Data from such thermocouples was not included in the temperature results after concluding obvious errors in the thermocouple connection or calibration.

5.2 CALCULATIONS

For each method, the respective equations are used to solve for thermal conductivity. The following figure shows an example of the change in thermal

conductivity over time with an AAC sample being tested in the Guarded Hot-Plate apparatus. Although the temperatures for the top and bottom plates are very similar, their difference in thickness yields slightly different values for thermal conductivity.

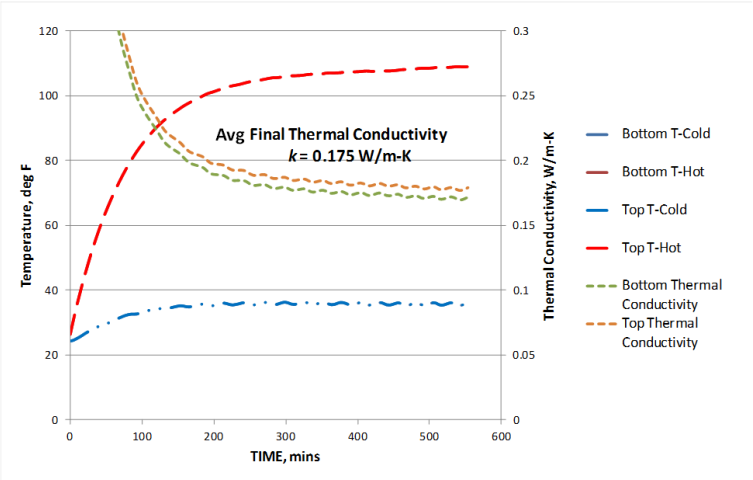

Figure 31: Graph of AAC Hot and Cold Temperatures and Thermal Conductivity Values

Once the final steady-state temperatures were recorded, a calculation was performed to take into account the heat lost through the 0.318 cm (0.125 in.) rubber pad. As found on Table 2, the thermal conductivity of the 1/8" pad at various compressions is shown. By using the actual thickness of the pad used in comparison with the resulting pad thickness, a compression percentage can be determined. A corresponding thermal conductivity of the compressed rubber pad can be used for additional testing and comparison. Since power remains constant and edge losses are considered negligible for this study, the heat transfer across the rubber pads will not affect the result.

GUARDED HOT-PLATE METHOD

As stated in Section 3.2, the thermocouples were placed in groups of six onto the 30 × 30 cm (12 × 12 in.) rubber pads, beginning with the bottom pad. The temperature values from the two thermocouples located in the primary guard portion of the rubber pad

were used to verify accuracy of the ultimate result, but were not averaged with the metered section readings.

The temperature values for each group of four thermocouples in the metered section were used to determine the average temperature for that side of the specimen. Values were checked for adherence to the 2% difference requirement and thermocouple errors were fixed or adjusted for proceeding runs whenever possible. Therefore, a total of four averaged temperatures from each test were obtained, two from the bottom specimen and two from the top specimen. Using Equation 10, the thermal conductivity was calculated over time until the steady state temperature was reached and the test was stopped.

If the temperature on the warmer side of the rubber pad is desired, the following calculations may be performed for the Guarded Hot-Plate. This is done by solving Equation 10 for the hotter side of the rubber pad, $T_{P,pad,hot}$ ('P' representing the value for the Guarded Hot-Plate, 'C' will be used for the Cylindrical Specimen). The equation for determining $T_{P,pad,hot}$ for the Guarded Hot-Plate is given by Equation 20.

$$T_{P,pad,hot} = \frac{Q_{heater}(x)}{2Ak_{pad}} + T_{P,pad,cool} \tag{20}$$

The final thermal conductivity for each test was obtained and recorded after a steady state temperature was established. The thermal conductivity values for tests performed on the Guarded Hot-Plate are shown in Table 3.

Table 3: Guarded Hot-Plate Thermal Conductivity Values

		Thermal Conductivity, W/m-K				
		1	2	3	4	Avg
Guarded Hot-Plate	Hardibacker	0.333				0.333
	Acrylite GP	0.185	0.192			0.189
	AAC	0.168	0.172			0.170
	AFRC	0.139	0.154	0.144	0.154	0.148
	FHWA	1.106	1.135			1.121

Due to the large difference in the first two tests for the AFRC samples, an additional two tests were ran to verify initial results. An analysis of the comparison between the thermal conductivity values of the Guarded Hot-Plate and Cylindrical Specimen methods is given in Section 5.3, Data Analysis.

CYLINDRICAL SPECIMEN METHOD

The insulation thermally isolates the top and bottom of the cylinder and reduces edge losses by a large amount. Carlson (2010) achieved a uniform one-directional heat flow in the radial direction in this manner. Therefore, Equation 19 provided by Carlson (2010) will be simplified by removing the edge loss term, Q_{loss}. This is shown in Equation 21.

$$k = \frac{(VI)\ln(r_2/r_1)}{2\pi L(T_1 - T_2)} \tag{21}$$

As with the Guarded Hot-Plate, the hotter side of the rubber pad nearest the cartridge heater, $T_{C,pad,hot}$, may be solved for in similar fashion as Equation 20. This is shown in Equation 22.

$$T_{C,pad,hot} = \frac{(VI)\ln(r_2/r_1)}{2\pi L k_{pad}} + T_{C,pad,cool} \tag{22}$$

In comparing the rubber pad compression between specimens, Appendix E shows the center hole diameter for the Acrylite® GP specimen to be smaller (2.49 cm) than that of the other specimens (2.72 cm) since it was cored by an offsite vendor. This ultimately also affects the compression of the 1/8" rubber pad, and its diameter is reduced by 0.27 cm.

Each test produced results from three possible specimens. A tolerance of 2% temperature difference between the inside- and outside-cylinder thermocouple groups

was maintained as with the Guarded Hot-Plate method. The following table shows the thermal conductivity values for all the tests performed on cylindrical specimens.

Table 4: Cylindrical Specimen Thermal Conductivity Values

		Thermal Conductivity, W/m-K				
		1	2	3	4	Average
Cylindrical Specimen	Hardibacker Backerboard	-				-
	Acrylite GP	0.1854	0.1859	0.1825	0.1830	0.1830
	AAC	0.1924	0.1842	0.1836	0.1833	0.1859
	AFRC	0.1675	0.1679			0.1677
	FHWA	1.0279	1.1414			1.0846

5.3 DATA ANALYSIS

Validation of Guarded Hot-Plate - The initial calibration of the Guarded Hot-Plate included comparisons with known samples of Hardibacker® Backerboard (ICC Evaluation Service Inc. 2004) and Acrylite® GP (TAP Plastics 2011). Table 5 shows their statistical comparison with the literature standard values.

Table 5: Calibration Samples Using the Guarded Hot-Plate Method

Guarded Hot-Plate	Avg Therm Cond, W/m-K	Literature Value, W/m-K	# Tests Ran	Standard Deviation	% Difference
Hardibacker Backerboard	0.333	0.33	1	0.00196	0.83%
Acrylite GP	0.189	0.19	2	0.00135	0.80%

Such a small standard deviation and percent difference between the found values and the literature values for both calibration samples provides reasonable assurance that the modified Guarded Hot-Plate can be relied upon to accurately measure the thermal conductivity of other types of materials.

Validation of Cylindrical Specimen Apparatus – The Acrylite® GP material was the only calibration sample used having a known thermal conductivity that could be fabricated

into the proper cylindrical shape. The following table shows the comparison of determined values with the literature values of Acrylite® GP (TAP Plastics 2011).

Table 6: Calibration Samples Using the Cylindrical Specimen Method

Cylidrical Specimen	Avg Therm Cond, W/m-K	Literature Value, W/m-K	# Tests Ran	Standard Deviation	% Difference
Acrylic GP	0.188	0.19	4	0.0018	1.05%

To improve the robustness of the Cylindrical Specimen apparatus, additional mixes of AFRC, AAC, and conventional concrete (FHWA) were used. Therefore, the values from the Guarded Hot-Plate apparatus are compared to determine the adequacy of the Cylindrical Specimen apparatus. Using Minitab, an Analysis Of Variance (ANOVA) is performed at a 95% confidence level. The box-plot statistical analysis of each mixture is shown in Figure 32, where 'P' represents the plate samples, and 'C' represents the cylindrical samples. Note that the FHWA values are shown on a separate axis.

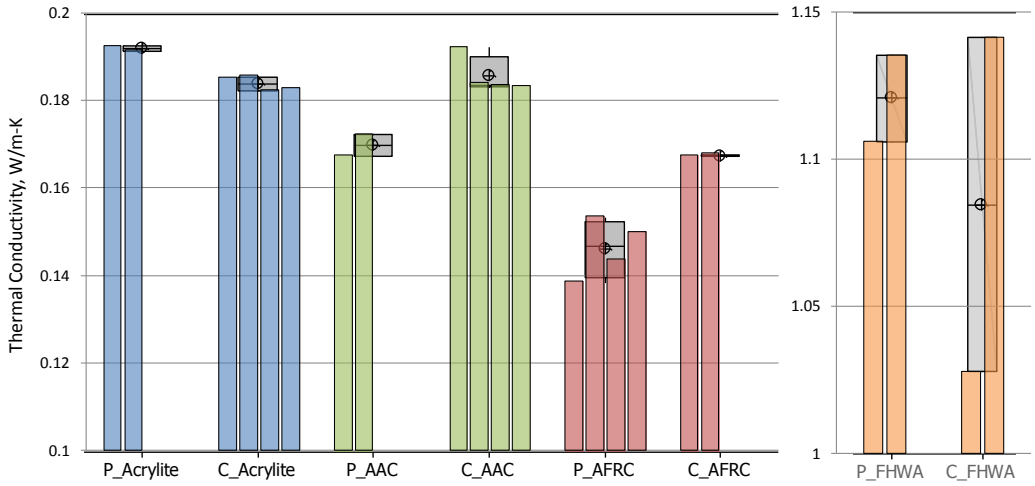

Figure 32: Graphic for Both Methods with Box-Plot Overlay

An additional output of the ANOVA process is shown in Figure 33, which compares the mixture means using the combined values of both testing methods.

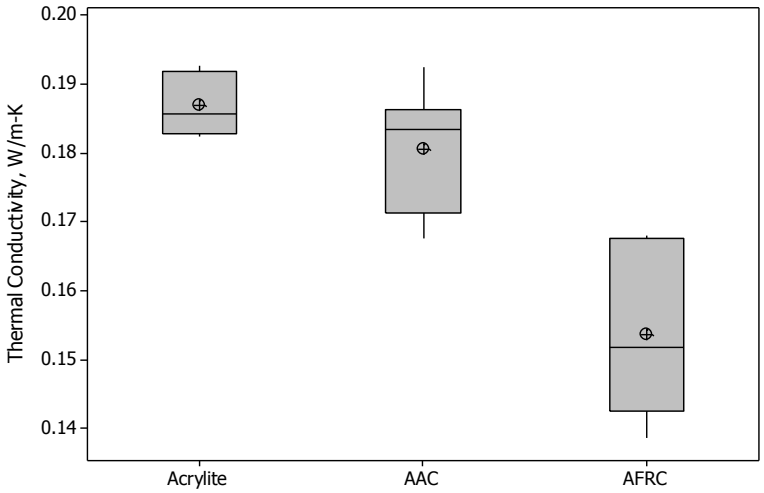

Figure 33: Variance Comparison of the Combined Means for Both Methods

Since the FHWA values are significantly greater, this comparison focuses on the variances of the three mixtures having similar thermal conductivity values. From Figure 33, the values from the Acrylite® GP and AAC samples are closest of the mixtures. Yet the values for AFRC are well below the Acrylite and AAC variances, including that of the FHWA mixture.

By using the P-values from ANOVA, an additional correlation can be drawn, as shown in Appendix F and as summarized in the following table.

Table 7: ANOVA P-Values Comparing Both Methods

	P-Value
Acrylite GP	0.004
AAC	0.012
AFRC	0.013
FHWA	0.600

Those with a P-value greater than 0.5 are considered to have a strong statistical correlation, and such is acceptable when using a 95% confidence interval. A loose correlation is assigned to samples having a P-value greater than 0.01. This reveals that

testing of the FHWA specimens logically produced a strong correlation between the two testing methods, while AAC and AFRC produced only better than a loose correlation.

As an additional means of comparing the data, the following figures show the graphical comparison of the values for both methods. Due to the significantly larger value for conventional concrete, Figure 35 removes the FHWA value to allow for another comparison of the Acrylite® GP, AFRC, and AAC results separately.

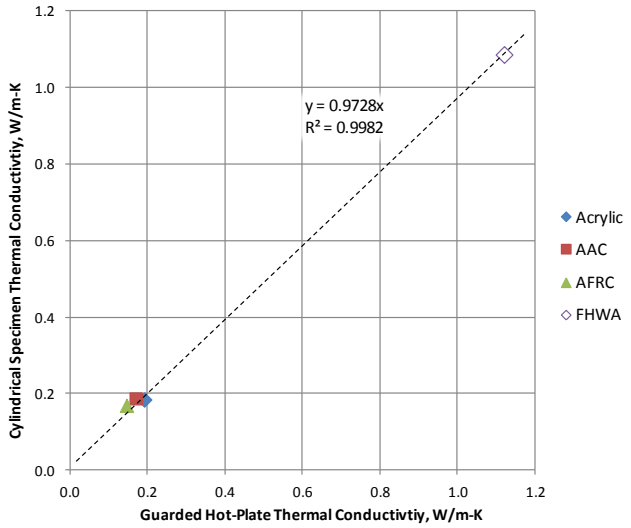

Figure 34: Graphical Comparison of Both Methods

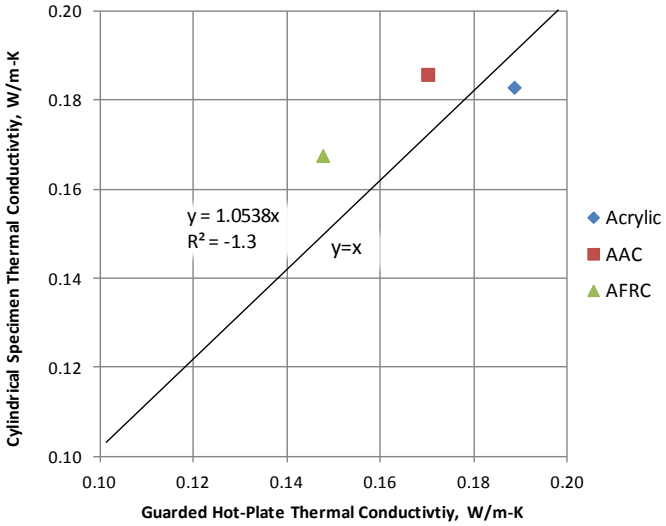

Figure 35: Graphical Comparison of Both Methods (FHWA Removed)

By using the 1:1 plot of Figure 34, the two methods resulted in a coefficient of determination R^2 of 0.9982, with the slope of 0.9728, meaning that the correlation between the values from the Guarded Hot-Plate tend to be slightly higher than those of the Cylindrical Specimen method. Yet, when analyzing the values with the distant FHWA value removed as in Figure 35, the Acrylite® GP thermal conductivity is slightly higher for the Guarded Hot-Plate method, and is the only mixture type below the equality line $y = x$. However, this plot also suggests that due to the very similar range of the thermal conductivity values of the three mixtures, a statistical correlation (with an intercept set to zero) based only on these three mixtures could not be established. A linear regression correlation of the three mixtures reveals that the fitted regression line does not accurately represent their thermal conductivity values.

Chapter 6

CONCLUSIONS AND RECOMMENDATIONS

6.1 CONCLUSIONS

By considering the test results obtained and statistical analysis performed, several conclusions may be drawn concerning the thermal conductivity data from the various mixtures. First, the percent difference values shown for the Guarded Hot-Plate in Table 5 are 0.83 and 0.80% for the Hardibacker® Backerboard and Acrylite® GP, respectively. These give strong evidence that the enhanced Guarded Hot-Plate apparatus in itself is an accurate measurement for thermal conductivity. Yet, those samples are homogeneous and contain no aggregates or various larger constituents that concrete mixtures often have.

When comparing the thermal conductivity values of the Guarded Hot-Plate to those of the enhanced Cylindrical Specimen method, the FHWA mixture provides, logically, the strongest correlation by having a larger thermal conductivity range compared to the other three mixtures. This was necessary to produce meaningful and accurate results. Although the standard deviation for the FHWA samples was larger than the other mixtures, the P-value of 0.600 gives additional confidence in the performance of the enhanced Cylindrical Specimen Apparatus for concretes possessing generally higher thermal conductivities. Unfortunately, the mixtures having a lower thermal conductivity did not have larger overlapping areas for the mean values of both testing methods, as shown in Figure 32. Nonetheless, a direct comparison of the absolute values and basic statistical variances give confidence in the repeatability and usefulness of the results.

Therefore, the modifications made for the Guarded Hot-Plate apparatus have been proven both through the use of two calibration samples and also by the strong

correlation for materials having a wider range of thermal conductivities. This is true even when the materials are non-homogeneous as with the case of the FHWA samples. The modifications made for the enhanced Cylindrical Specimen apparatus also provide confidence with materials having a higher thermal conductivity. Excepting the P-value for Acrylite® GP, the modifications provide a P-value of at least 0.01 for materials having values in the range of the Hardibacker® Backerboard, AFRC, and AAC thermal conductivity values (0.13 to 0.33 W/m-K), as can be seen in Appendix F in the ANOVA calculations for each mixture.

6.2 RECOMMENDATIONS FOR FUTURE APPLICATION

With the largest investment of time allocated to the development of both enhanced apparatus, and limited availability of different mixture types, insufficient time was spent in testing. Therefore, the need for additional repeated tests would benefit the validation of both the enhanced Guarded Hot-Plate and Cylindrical Specimen apparatus. Also, experimenting with a variety of power inputs would create smaller or larger temperature gradients across each specimen thickness. This would provide additional evidence for initial thermal conductivity values. Noting the large gap between the FHWA samples and those with lower thermal conductivity values, additional mixtures having a wider thermal conductivity within the range of 0.33 to 1.02 W/m-K would provide additional confidence for using these methods.

Lastly, both methods would benefit by having similar samples made with different thicknesses. The ASTM Guarded Hot-Plate procedure recommends a maximum specimen thickness of one-third the maximum linear dimension of the metered section. Yet the limiting range of slab thickness could be confirmed to determine the point at which thermal conductivity measurements become inconsistent. Similarly, specimens

having different radii may be investigated. In addition, another standard cylindrical geometry may be used, such as 15 × 30 cm (6 × 12 in.) cylinders. If other radii are explored, the ASTM C 177-04 recommendation of a minimum width-to-thickness ratio of 3 to 1 should be maintained. Also, as stated by Carlson (2010), an appropriate radius is one that is at least twice the diameter of the material's largest aggregate size.

Since the influence that moisture content has on the specimens was minimized by drying the specimens in an 80^{o}C oven for 48 hours, an additional measurement may be made. To determine the thermal conductivity of the material in its placed setting, the specimens would be tested without drying. This would mean testing at a lower range of temperatures since, at temperature above 100^{o}C, the phase change of water from liquid to steam will have a detrimental influence on the results. This would provide a more accurate depiction of how the material will behave after placement in its structure.

Guarded Hot-Plate Recommendations - Due to the slight variations in the surface of samples, a light grinding of certain samples would have provided a flatter surface for testing. Although caution must be taken with denser concretes, grinding away rough outer edges would also allow for a snug fit of the foam insulation around the circumference of the apparatus. To determine the sensitivity of the apparatus to the effectiveness of the heat sink, the cooling fans may be adjusted in speed or turned off all together. While it is not strictly enforced by the ASTM guideline how heat transfer from the slabs is accomplished, their effectiveness could be considered.

Cylindrical Specimen Recommendations - A large source of difficulty came only after repeated testing when the thermocouple rods began breaking near the tip that holds the thermocouple junction, as shown in Figure 24. This could be resolved by using a stronger

material for the rod that has a reasonably low thermal conductivity as not to affect heat transfer from the cylinder.

Another problem arose after repeated testing. Although only a few seconds are required for cleanup, if neglected over time, the thermocouple tips become covered with thermal paste that becomes more firm and obstructs the solid contact with the surface of the cylinder. This would be facilitated by providing more room between the cylinder surface and V-shaped bars, and could be accomplished by either spreading the three dowel rods further apart, or by fabricating the V-shaped bars with a larger interior angle. Other than these adjustments, switching of samples was quite efficient and simple.

The cylindrical sample of Acrylite® GP gave the best snug fit for the rubber pad and cartridge heater. Perhaps this was due to their manufacturers coring it with a slightly smaller diameter, 2.49 cm, than the requested 2.54 cm (1 in.) diameter. Occasionally for the other samples with a 2.72 cm diameter, the rubber pad and cartridge heater did not fit as snug as would be desired to preclude any air voids from existing between the cartridge heater and cylinder wall. This may be facilitated by either having a spacer that has a similar thermal conductivity as the rubber pad, or by obtaining similar type rubber pads with a thickness of 0.63 cm (0.25 in.). These sizes were initially attempted but proved too thick to allow the cartridge heater to be rotated into place. Though it required experience and a little more patience, the ultimate solution for cylinders with the slightly larger radii was to layer the 0.318 cm (0.125 in.) thick pad with a 0.159 cm (0.063 in.) thick pad before insertion into the cylinder. No sizes were available similar to this "in-between" thickness created by layering the two pads. When switching the thicknesses of the pads, more care should be taken in estimating the compression percentage and corresponding thermal conductivity, as shown in Table 2. This must then be translated into the proper power reduction for the overall test run.

REFERENCES

ASTM C 1386-07. (2007). *Standard Specification for Precast Autoclaved Aerated Concrete (AAC) Wall Construction Units*. PA.

ASTM C 177-97. (2003). *Standard Test Method for Steady-State Heat Flux Measurements and Thermal Transmission Properties by Means of the Guarded-Hot-Plate. Practice*, 22.

Alajlan, S. (2006). "Measurements of thermal properties of insulation materials by using transient plane source technique." *Applied Thermal Engineering*, 26(17-18), 2184-2191.

Arctic Silver. (2011). "Arctic Silver Thermal Adhesive." <http://arcticsilver.com/arctic_silver_thermal_adhesive.htm> (Aug. 15, 2011).

Bonakdar, A., and Mobasher, B. (2010). *Analysis of Thermal Properties of Aerated Fiber Reinforced Concrete systems*. Arizona State University, Tempe, AZ.

Carlson, J. D., Bhardwaj, R., Phelan, P. E., Kaloush, K. E., and Golden, J. S. (2010). "Determining Thermal Conductivity of Paving Materials Using Cylindrical Sample Geometry." *ASCE Journal of Materials in Civil Engineering*, 22(2), 186-195.

Chong, U. (2006). "Thermal Conductivity of Construction Materials." Arizona State University, Tempe, AZ.

Golden, J. (2004). "The Built Environment Induced Urban Heat Island Effect in Rapidly Urbanizing Arid Regions - A Sustainable Urban Engineering Complexity." *Journal of Integrative Environmental Sciences*, 1(4), 321-349.

Gustafsson, S. E. (1991). "Transient plane source techniques for thermal conductivity and thermal diffusivity measurements of solid materials." *American Institute of Physics*, 797-805.

Holt, E., and Raivio, P. (2005). "Use of gasification residues in aerated autoclaved concrete." *Cement and Concrete Research*, 35(4), 796-802.

Hukseflux. (2011). "Thermal Conductivity Measurement." <http://www.hukseflux.com/thermalScience/thermalConductivity.html> (2010).

ICC Evaluation Service Inc. (2004). *Legacy Report NER-405*. Fontana, California.

Kaloush, K. E., Carlson, J., Golden, J. S., and Phelan, P. E. (2008). *The Thermal and Radiative Characteristics of Concrete Pavements in Mitigating Urban Heat Island Effects*. Arizona State University, Tempe, AZ.

Luca, J., and Mrawira, D. (2005). "New Measurement of Thermal Properties of Superpave Asphalt Concrete." *Journal of Materials*, 17(1), 72-79.

Mehta, B. Y. P. K. (2002). “Greening of the Concrete Industry for Sustainable Development.” *Concrete International*, (July), 23-28.

Mrawira, D. M., and Luca, J. (2002). “Thermal Properties and Transient Temperature Response of Full-Depth Asphalt Pavements.” *Transportation Research Record: Journal of the Transportation Research Board*, 1809, 160-171.

Saint-Gobain Performance Plastics. (2010). “Thermally Conductive Silicone Sponge.” Hoosick Falls, NY.

TAP Plastics. (2011). “Physical Properties of Acrylite GP Acrylic Sheet.” <http://www.tapplastics.com/info/acrylic.php?#GP> (Sep. 13, 2011).

Tada, H. (2002). “Overview of Heat Transfer.” <http://www.tufts.edu/as/tampl/en43/lecture_notes/ch1.html> (Sep. 20, 2011).

Tan, S., Low, B., and Fwa, T. (1992). “Determination of thermal conductivity and diffusivity by transient heating of a thin slab.” *Building and Environment*, 27(1), 71-76.

Witczak, M. W., Kaloush, K., Pellinen, T., El-Basyouny, M., and Von Quintus, H. (2002). *Simple Performance Test for Superpave Mix Design*. Washington, D.C.

Young, H. D. (1992). *University Physics*. Addison Wesley.

Zhu, D., Bonakdar, A., Morris, D., Kaloush, Kamil, and Mobasher, B. (2010). *Analysis of Mechanical Properties, Structural Response, and Thermal Properties of Composite Wall Systems*.

Çengel, Y. A. (2003). *Heat Transfer*. McGraw Hill, New York, NY.

APPENDIX A

GUARDED HOT-PLATE APPARATUS DIMENSIONS

The following are Figures generated by Chong (2006), since his center plates were utilized in the enhanced Guarded Hot-Plate apparatus development.

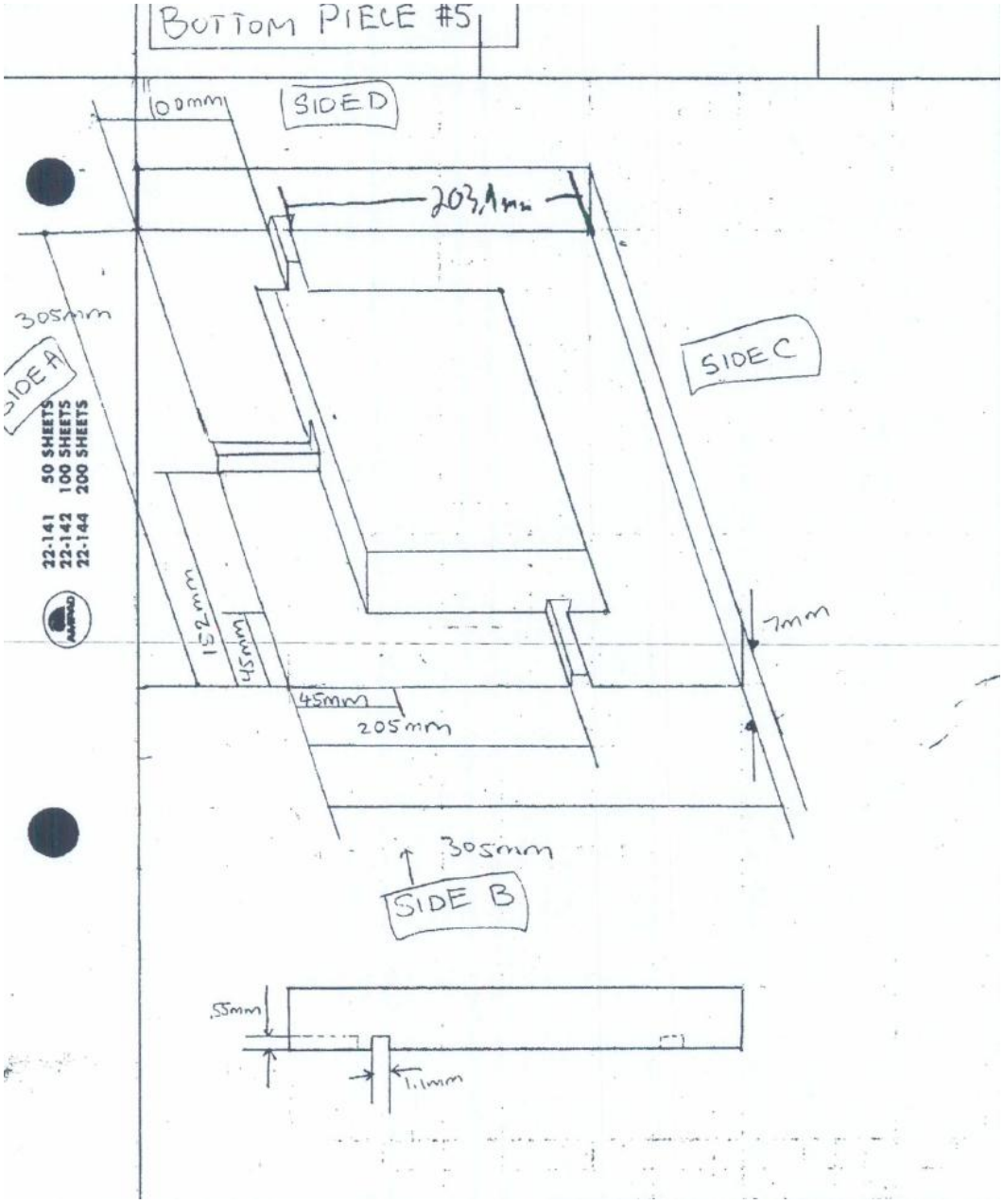

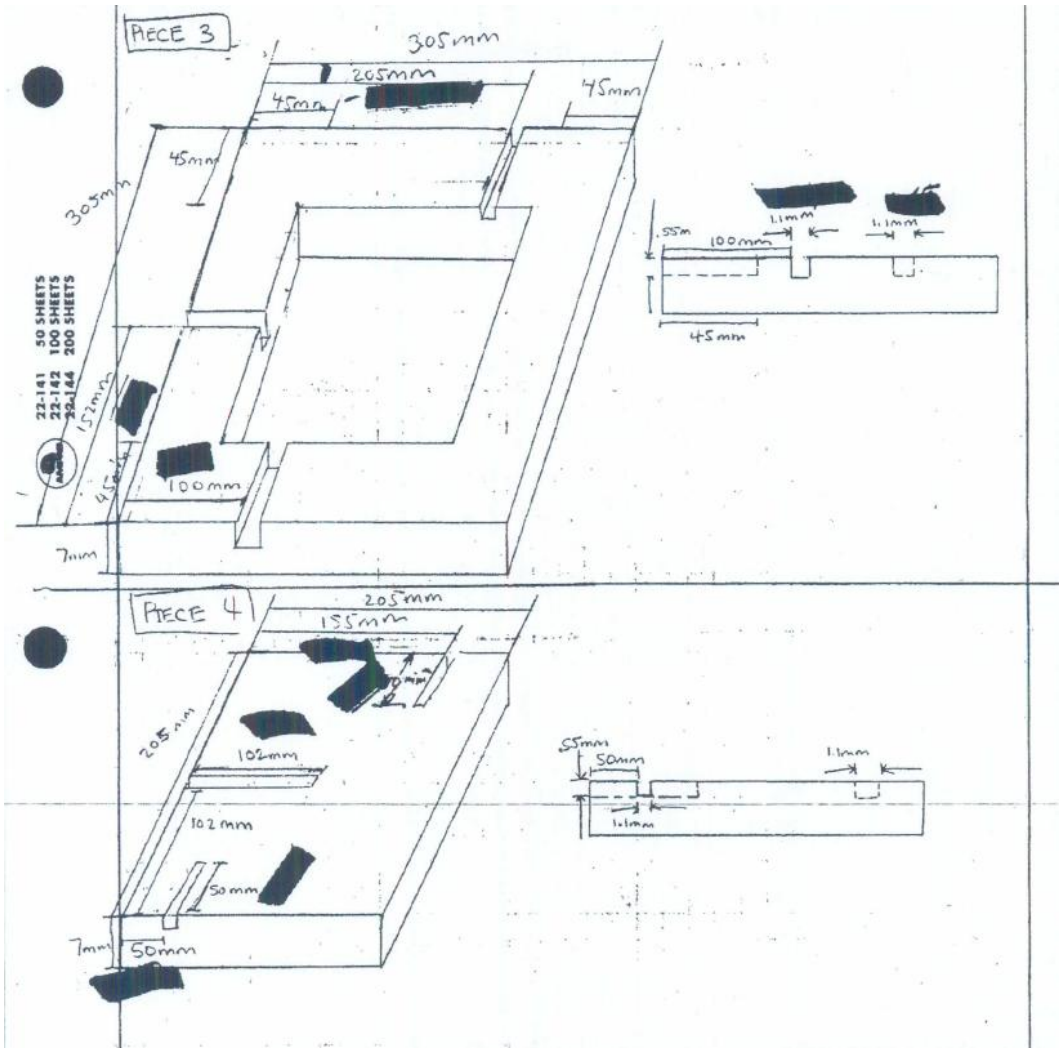
PIECE 3
305mm
205mm
45mm
45mm
45mm
305mm
152mm
100mm
7mm
.55m
100mm
1.1mm
1.1mm
45mm
22-141 50 SHEETS
22-142 100 SHEETS
22-144 200 SHEETS
PIECE 4
205mm
155mm
205mm
102mm
102mm
50mm
7mm
50mm
55mm
50mm
1.1mm
1.1mm

APPENDIX B

CYLINDRICAL SPECIMEN APPARATUS DIMENSIONS

Figure B-1: A side view of the cylindrical apparatus, showing vertical dimensions including location of inner thermocouples (red dots) and estimated locations of outer thermocouples (red 'x', light colored on backside of sample).

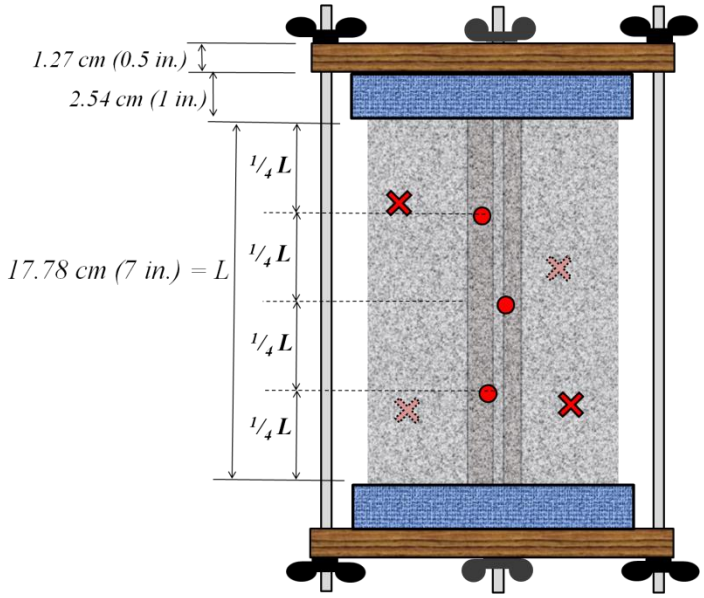

Figure B-2: Top view of cylinder and V-shaped bars. The 0.64 cm (0.25 in.) diameter metal dowel rods are shown as being inside the

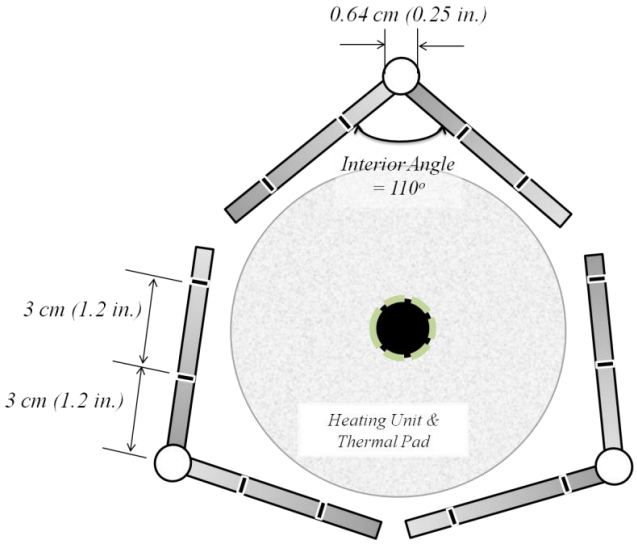

Figure B-3: Triangular Board for top; bottom triangular board does not need the center cut burg4since this is for the cartridge heater exit wires.

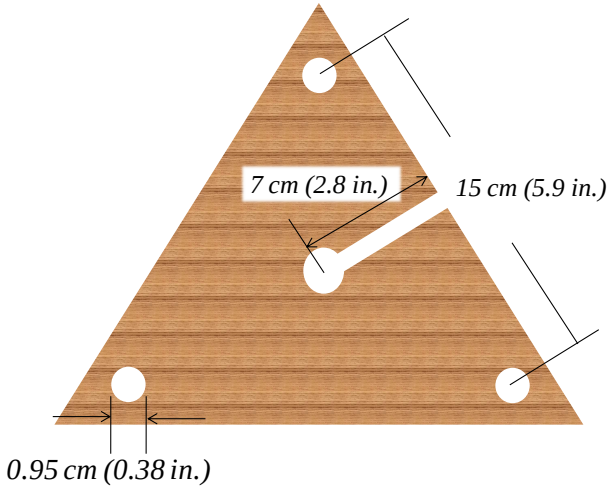

APPENDIX C

GUARDED HOT-PLATE TESTING PROCEDURE

1. Power Source:
    1.1. Assure that variac (power source) is off during setup
    1.2. Assure that main heater is properly connected to the variac power source
    1.3. Assure that primary guard heaters are properly connected in parallel to power source
    1.4. Assure that voltmeters are in parallel with circuit for reading during test (although this can be obtained during test without prior placement)
    1.5. Assure that ammeter is in series with the main heater circuit for current readings
        1.5.1. Turn ammeter on only when taking readings to conserve battery life
2. Flat Plate Specimen:
    2.1. Take Measurements
        2.1.1. Record measurements of width and depth (in cm)
        2.1.2. Record 2 measurements of thickness (in cm) on opposite sides of sample
        2.1.3. Record weight (in grams). This will be considered the non-dry weight used in calculating mixture moisture content
    2.2. Dry in Oven
        2.2.1. Place in oven at 80^{o}C for approximately 48 hours
        2.2.2. Remove samples from oven and cool for approximately 2 hours before testing. Cooling time may vary depending on the density of samples
        2.2.3. Record dry weight of sample as soon as cool enough to handle
        2.2.4. Calculate and record moisture content of sample using Equation 3
3. Thermocouples placement on thermal pads:
    3.1. Place thermocouples on four rubber pads as shown in Figure 16 using Kapton® tape

3.1.1. Place the first four thermocouples in the main heater area of the thermal pad, keeping all at least 1.27 cm (0.5 in.) from the edge of the area

3.1.2. Place the next two thermocouples in the primary guard area of the thermal pad, similarly keeping both 1.27 cm (0.5 in.) from the edge of the plate

3.1.3. Rubbing Kapton® tape with a hard edge may be used to improve its adhesion to rubber pad

3.2. Repeat process for other three thermal pads, maintaining randomness of thermocouple placement within aforementioned boundaries

3.3. Label each thermocouple with its respective DAQ channel for accurate identification and replacement if needed

4. Placement of Kapton® Heaters:

4.1. Once bottom half of assembly is in place, put metered heater squarely over metered plate and use Kapton® tape to keep in place

4.2. Place four primary guard heaters on each side of primary guard plate, centering them on their respective side, using Kapton® tape to keep them in place

4.3. Coordinate lead wires from each heater to go inside designated grooves of each plate

5. Apparatus Assembly for Testing:

5.1. Place bottom copper plate, with cooling fans face down, on top of support structure. All following layers will remain square with the edges of this first layer

5.2. Place first rubber pad on top of bottom copper plate with the thermocouple-side face up

5.3. Place one-of-two samples on top of rubber pad

5.4. Place second rubber pad on top of the sample with the thermocouple-side face down toward the sample

5.5. Place the first layer of the center copper plates having the Kapton® Heaters on them next, keeping the prescribed 0.5 cm (0.2 in.) gap between the center plate and primary guard plate

5.6. Place the top layer of the center copper plates, lining up heater wire grooves with bottom layer of center copper plate to assure minimal air gap between center plates

5.7. Place next layers containing the third rubber pad, specimen, fourth rubber pad, and top copper plate with cooling fans face up, symmetric to the bottom portion of the apparatus

6. Placement of Foam Insulation and Clamps:

6.1. Strap foam around apparatus, being careful to keep non-heat resistant wires outside of the foam

6.1.1. The high gauge of the thermocouples minimizes the creation of gap on outer circumference of apparatus and they can simply be bent to fit under the foam

6.2. Place clamps on each of the four corners, approximately an in. from the edges if possible

6.2.1. Tighten the clamps only enough to make apparatus snug

6.2.1.1. If excessively compressed on corners, adhesion of thermal paste will break between cooling fans and outer copper plates

7. Turning on Power and DAQ:

7.1. Turn on National Instruments DAQ

7.2. On computer, start LabView file

7.2.1. Switch to appropriate Hot-Plate tab

7.2.2. Click “RUN” button at top left and wait 60 seconds for first data point to register

7.2.3. Save file as appropriate

7.3. Turn on variac power for primary guard heaters and then for the main heater

7.3.1. These may overdraw current if turned on simultaneously, allow for several seconds between turning each on to allow surge current to settle

7.3.2. During testing, assure that the temperature values of the primary guard heaters remain within 2% of the temperature values of the main heater thermocouples on the hot side of the specimen

8. Intermediate and Finish:

8.1. Record Voltage (V), Current (A), and (for reference) the variac % reading at beginning and near end of experiment

8.2. Allow to run until steady state temperature is reached (at least 4 hours)

8.3. Press “STOP” button on LabView

8.4. Turn off power to DAQ, ammeters & voltmeters, and variac

8.5. Allow to cool before dismantling apparatus

9. Data Transfer:

9.1. Copy and Paste data containing file into Excel Guarded Hot-Plate Template

9.2. Fill in appropriate information and recorded measurements

9.3. Calculate the thermal conductivity for top and bottom samples, averaging the two values to determine a final value of the test

APPENDIX D

CYLINDRICAL SPECIMEN TESTING PROCEDURE

1. Power Source:
    1.1. Assure that variac (power source) is off during setup
    1.2. Assure that cylinder heaters are properly connected to the variac power source
    1.3. Assure that voltmeters are in parallel with circuit for reading (although this can be checked during the experiment manually)
    1.4. Assure that ammeter is in series with one of the three experiment specimen cartridge heaters for current reading
        1.4.1. Turn on only when taking readings to conserve battery life
2. Cylinder:
    2.1. Take Measurements
        2.1.1. Record measurements from the inner radius to the outer radius (2 on top and 2 on bottom) (in cm)
        2.1.2. Record 2 measurements of height (in cm)
        2.1.3. Record weight (in grams). This will be considered the non-dry weight used in calculating mixture moisture content
    2.2. Dry in Oven
        2.2.1. Place in oven at 80^{o}C for approximately 48 hours
        2.2.2. Remove samples from oven and cool for approximately 2 hours before testing. Cooling time may vary depending on the density of samples
        2.2.3. Record dry weight of sample as soon as cool enough to handle
        2.2.4. Calculate and record moisture content of sample using Equation 3
3. Thermocouples placement:
    3.1. Lengthen first three thermocouples into and through to the bottom of the center hole so they come through the bottom plane of the cylinder

3.2. Assure that next four thermocouples are placed on stand and that their ends are bent around tips of plastic rods to give good contact with cylinder surface

3.3. Remaining thermocouples may be used for ambient temperature measurement

4. Placement of rubber pad

4.1.1. Cut rubber pad to completely wrap the inner circumference of the center hole while not protruding outside the top and bottom of the cylinder

4.1.2. Rubber pad may have to be rolled tightly and turned back and forth as it is placed in the hole

4.1.3. Assure the edges of the TP from top to bottom of cylinder are closed and flush with the top and bottom of the cylinder

4.1.3.1. Attempt to place thermocouples randomly around the center hole circumference

4.1.4. While pulling up on the three thermocouples placed in the center hole, pull each thermocouple beginning with CH0 through CH2 so first is approximately a quarter-way from the bottom, the second thermocouple is halfway, and the third thermocouple is three-quarters of the way from the bottom

4.1.4.1. This provides a good average of the temperature that the heater imposes on the cylinder sample

5. Cylindrical Heater:

5.1.1. Take caution not to pull on the power wires coming from heater

5.2. Press heater into center hole, twisting as needed

5.2.1. Assure that thermocouples remain in place while placing the heater to protect delicate thermocouple tip junctions

6. Placing Cylinder

6.1. Place and center the cylinder on top of 2.54 cm (1 in.) foam insulation on stand, careful not to break off the thermocouple holding rods

6.2. Insert small foam wedges on the end opposite each thermocouple in the V-shaped bars on the stand. This provides good contact with the thermocouple firmly against the cylinder surface and ensures good contact.

6.2.1. Place an amount of Thermal Paste on cylinder where each thermocouple makes contact, assuring that the entire thermocouple tip is enclosed by Thermal Paste (Thermal Paste does not dry, and will drip during experiment if too much is applied)

6.3. Put Styrofoam on top of cylinder and check for a good fit before pressing on triangular wood cap

6.4. Screw down the top triangular board using the wing nuts so the cylinder is snug and devoid of air gaps

7. Turning on Power and DAQ:

7.1. Turn on National Instruments DAQ

7.2. On computer, start LabView file

7.2.1. Switch to appropriate Cylinder tab

7.2.2. Click "RUN" button at top left and wait 60 seconds for first data point to register

7.2.3. Save file as appropriate

7.3. Turn on variac power for primary guard heaters and then for the main heater

7.3.1. These may overdraw current if turned on simultaneously, allow for several seconds between turning each on to allow surge current to settle

8. Intermediate and Finish:

8.1. Record Voltage (V), Current (A), and the variac % reading (for reference) at beginning and near end of experiment

8.2. Allow to run until steady state temperature is reached (at least 4 hours)

8.3. Press “STOP” button on LabView

8.4. Turn off power to DAQ, ammeters & voltmeters, and variac

8.5. Allow to cool before dismantling apparatus

9. Data Transfer:

9.1. Copy and Paste data containing file into Excel Cylindrical Specimen Template

9.2. Fill in appropriate information and recorded measurements

9.3. Calculate the thermal conductivity for samples

APPENDIX E

SAMPLE DIMENSIONS AND PROPERTIES

The two samples made for AFRC are labeled as _1 and _2

Guarded Hot-Plate											
Mixture Type	Sample	dried weight, g	non-dry weight, g	moisture content, %	length, cm	width, cm	thick_1, cm	thick_2, cm	thick_avg, cm	Volume, cm^3	density, g/cm^3
Acrylite GP	1	*(not dried)*	2841	-	30.5	30.4	2.5	2.5	2.54	2355	1.206
	2	*(not dried)*	2781	-	30.5	30.4	2.6	2.6	2.57	2379	1.169
HardiBacker®	1	1123	1150	2.35	30.5	30.4	1.0	1.0	1.02	942	1.192
	2	1103	1119	1.43	30.4	30.4	1.0	1.0	1.04	962	1.146
AFRC_1	1	1056	1083	2.44	30.2	30.0	2.0	2.0	1.96	1777	0.595
	2	1053	1082	2.72	30.0	30.2	2.0	2.0	1.97	1782	0.591
AFRC_2	1	1294	1321	2.03	30.2	30.0	2.6	2.5	2.54	2301	0.562
	2	1280	1314	2.61	30.0	30.2	2.6	2.4	2.53	2290	0.559
AAC	1	1265		-	29.8	29.9	2.4	2.3	2.36	2106	0.601
	2	1329		-	29.9	29.8	2.4	2.6	2.47	2196	0.605
FHWA	1	5995	5960	-0.59	30.5	30.4	2.8	2.9	2.84	2629	2.280
	2	6745	6775	0.44	30.3	30.8	3.1	3.1	3.12	2916	2.313

There are two samples for each mixture, shown as #1 and #2, excepting the Acrylite® GP. The respective thickness 1 & 2 for the top and bottom of the specimen are measured at 180° from each other at the most visibly off-centered location of the hole's exit point.

Cylindrical Specimen									
					TOP		BOTTOM		
Mixture Type	non-dry weight, g	height, cm	diam, cm	center, cm	thickness 1, r1-r2, cm.	thickness 2, r1-r2, cm.	thickness 1, r1-r2, cm.	thickness 2, r1-r2, cm.	avg thickness, cm
Acrylite GP	1575.1	17.86	10.08	2.49	3.84	3.78	3.81	3.78	3.80
AAC#1	772.8	17.86	10.31	2.72	3.78	3.68	3.51	3.68	3.66
AAC#2	788.7	17.68	10.21	2.72	3.68	3.73	3.76	3.56	3.68
AFRC#1	799.2	17.86	9.98	2.72	3.63	3.66	3.66	3.66	3.65
AFRC#2	785.7	17.68	9.88	2.72	3.58	3.58	3.68	3.63	3.62
FHWA#1	3095.5	17.88	10.31	2.72	3.71	3.94	3.66	3.96	3.82
FHWA#2	3109.4	17.75	10.21	2.72	3.91	3.66	3.30	4.22	3.77

APPENDIX F

THERMAL CONDUCTIVITY CALCULATIONS

GUARDED HOT-PLATE

An example of the calculations for the thermal conductivity of Acrylite® GP using Equation 10, $k = \frac{Q_{heater}(x)}{2A(T_1 - T_2)}$, with colored cells representing calculations. This is followed by the calculated values for each mixture type.

A-1	B-1	C-1	D-1
2	***Guarded Hot-Plate - Acrylite GP***		
3	***Acrylite GP***	***#1***	
4	Thickness (m)	0.0254	0.0254
5	Cross Section Area (m^2)	0.04129	0.04129
6	Voltage (Volts)	42.3	
7	Current (A)	1.042	
8	Total Power (V*A)	=C6*C7	
9	Pads = 96% Power	=C8*0.96	
10	Thot (^oC)	112.957	112.554
11	Tcold (^oC)	42.623	47.584
12	Temp Change (K)	=C10-C11	=D10-D11
13	Thermal Conductivity (W/m-K)	=C9*C4/C5/C12/2	=C9*D4/D5/D12/2
14	**Individual Average**	=AVERAGE(C13:D13)	

Guarded Hot-Plate - HardiBacker		
Hardibacker (R) BackerBoard	***#1***	
Thickness (m)	0.0213	0.0213
Cross Section Area (m^2)	0.0413	0.0413
Voltage (Volts)	42.6	
Current (A)	1.042	
Total Power (V*A)	42.70	
Thot (^oC)	65.7	65.2
Tcold (^oC)	34.7	29.7
Temp Change (K)	31.0	35.5
Thermal Conductivity ($WK^{-1}m^{-1}$)	0.356	0.310
Individual Average	0.333	

Guarded Hot-Plate - Acrylite GP				
Acrylite GP	***#1***		***#2***	
Thickness (m)	0.0254	0.0254	0.0254	0.0254
Cross Section Area (m^2)	0.0413	0.0413	0.0413	0.0413
Voltage (Volts)	40.6		40.9	
Current (A)	1.042		1.044	
Total Power (V*A)	42.31		42.70	
Thot (^oC)	113.0	112.6	115.2	114.7
Tcold (^oC)	42.6	47.6	42.5	49.9
Temp Change (K)	70.3	65.0	72.7	64.8
Thermal Conductivity (W/m-K)	0.178	0.192	0.181	0.203
Individual Average	0.185		0.192	

Guarded Hot-Plate - AAC				
AAC	***#1***		***#2***	
Thickness (m)	0.0236	0.0247	0.0161	0.0170
Cross Section Area (m^2)	0.0413	0.0413	0.0413	0.0413
Voltage (Volts)	40.5		40.5	
Current (A)	1.032		1.032	
Total Power (V*A)	41.79		41.79	
Thot (^oC)	108.7	108.7	85.9	85.9
Tcold (^oC)	35.8	35.8	36.4	36.4
Temp Change (K)	72.9	72.9	49.6	49.6
Thermal Conductivity (W/m-K)	0.164	0.171	0.165	0.173
Individual Average	0.168		0.172	

Guarded Hot-Plate - AFRC								
AFRC	***#1***		***#2***		***#3***		***#4***	
Thickness (m)	0.0196	0.0197	0.0196	0.0197	0.0254	0.0253	0.0254	0.0253
Cross Section Area (m^2)	0.0413	0.0413	0.0413	0.0413	0.0413	0.0413	0.0413	0.0413
Voltage (Volts)	40.4		40.4		40.9		41.9	
Current (A)	1.040		1.039		1.044		1.044	
Total Power (V*A)	42.03		41.99		42.70		43.74	
Thot (^oC)	108.8	108.8	99.9	99.9	131.1	129.3	126.9	124.7
Tcold (^oC)	36.7	36.7	34.8	34.9	39.7	38.4	39.0	37.9
Temp Change (K)	72.2	72.1	65.0	65.0	91.4	90.9	87.9	86.8
Thermal Conductivity (W/m-K)	0.138	0.139	0.153	0.154	0.144	0.144	0.153	0.154
Individual Average	0.139		0.154		0.144		0.154	

CYLINDRICAL SPECIMEN

An example of the calculations for the thermal conductivity of Acrylite® GP using Equation 21, $k = \frac{(VI)\ln(\mathbf{r_2}/\mathbf{r_1})}{2\pi L(T_1 - T_2)}$, with colored cells representing calculations. This is followed by the calculated values for each mixture type.

A-1	B-1	C-1
2	***Cylinder - Acrylite GP***	
3	***Acrylite GP***	***#1***
4	Radius, Past Heater, r1 (m)	0.009525
5	Radius, Past Pad, r2 (m)	0.0127
6	Radius, Past Cylinder, r3 (m)	0.0381
7	Cylinder Length, L (m)	0.1778
8	Voltage (Volts)	19.98
9	Current (A)	0.72
10	Total Power (V*A)	=C8*C9
11	Pads = 96% Power	=C10*0.96
12	Thot (^{o}C)	127.447710059156
13	Tcold (^{o}C)	34.9948291731537
14	Temp Change (K)	=C12-C13
15	Thermal Conductivity (W/m-K)	=(C11*LN(C6/C4))/(2*3.14159*C7*(C12-C13))

Cylinder - Acrylite GP				
Acrylite GP	***#1***	***#2***	***#3***	***#4***
Radius, Past Heater, r1 (m)	0.0095	0.0095	0.0095	0.0095
Radius, Past Pad, r2 (m)	0.0125	0.0125	0.0125	0.0125
Radius, Past Cylinder, r3 (m)	0.0380	0.0380	0.0380	0.0380
Heater Cylinder Length, L (m)	0.1778	0.1778	0.1778	0.1778
Voltage (Volts)	19.18	19.18	19.18	19.18
Current (A)	0.72	0.72	0.72	0.72
Total Power (V*A)	13.81	13.81	13.81	13.81
Thot (^{o}C)	127.4	127.4	128.2	128.5
Tcold (^{o}C)	35.0	35.2	34.3	34.9
Temp Change (K)	92.5	92.2	93.9	93.7
Thermal Conductivity (W/m-K)	0.185	0.186	0.182	0.183

Cylinder - AAC				
AAC	***#1***	***#2***	***#3***	***#4***
Radius, Past Heater, r1 (m)	0.0095	0.0095	0.0095	0.0095
Radius, Past Pad, r2 (m)	0.0127	0.0127	0.0127	0.0127
Radius, Past Cylinder, r3 (m)	0.0381	0.0381	0.0381	0.0381
Heater Cylinder Length, L (m)	0.1778	0.1778	0.1778	0.1778
Voltage (Volts)	19.18	19.18	19.18	19.18
Current (A)	0.72	0.72	0.72	0.72
Total Power (V*A)	13.81	13.81	13.81	13.81
Thot (^{o}C)	121.3	129.3	125.0	128.4
Tcold (^{o}C)	32.2	36.2	31.6	34.9
Temp Change (K)	89.1	93.1	93.3	93.5
Thermal Conductivity (W/m-K)	0.192	0.184	0.184	0.183

Cylinder - AFRC		
AFRC	***#1***	***#2***
Radius, Past Heater, r1 (m)	0.0095	0.0095
Radius, Past Pad, r2 (m)	0.0127	0.0127
Radius, Past Cylinder, r3 (m)	0.0381	0.0381
Heater Cylinder Length, L (m)	0.1778	0.1778
Voltage (Volts)	19.18	19.18
Current (A)	0.72	0.72
Total Power (V*A)	13.81	13.81
Thot (^{o}C)	136.1	136.1
Tcold (^{o}C)	33.7	34.1
Temp Change (K)	102.3	102.0
Thermal Conductivity (W/m-K)	0.167	0.168

Cylinder - FHWA		
FHWA	***#1***	***#2***
Radius, Past Heater, r1 (m)	0.0095	0.0095
Radius, Past Pad, r2 (m)	0.0127	0.0127
Radius, Past Cylinder, r3 (m)	0.0381	0.0381
Heater Cylinder Length, L (m)	0.1778	0.1778
Voltage (Volts)	19.18	19.18
Current (A)	0.72	0.72
Total Power (V*A)	13.81	13.81
Pads = 96% Power	13.26	13.26
Thot (^{o}C)	53.9	53.3
Tcold (^{o}C)	37.2	38.3
Temp Change (K)	16.7	15.0
Thermal Conductivity (W/m-K)	1.028	1.141

An Analysis Of Variance (ANOVA) is shown for each mixture type comparing the two testing methods (P = Plate specimens, C = Cylindrical specimens). (Note the P-value.)

One-way ANOVA: P_Acrylite, C_Acrylite

```
Source  DF         SS         MS      F      P
Factor   1  0.0000847  0.0000847  35.99  0.004
Error    4  0.0000094  0.0000024
Total    5  0.0000942

S = 0.001534   R-Sq = 90.00%   R-Sq(adj) = 87.50%


Level       N     Mean    StDev
P_Acrylite  2  0.19216  0.00073
C_Acrylite  4  0.18419  0.00172


            Individual 95% CIs For Mean Based on Pooled StDev
Level         +---------+---------+---------+---------
P_Acrylite                      (--------*--------)
C_Acrylite    (-----*-----)
              +---------+---------+---------+---------
            0.1820    0.1855    0.1890    0.1925

Pooled StDev = 0.00153
```

One-way ANOVA: P_AAC, C_AAC

```
Source  DF         SS         MS      F      P
Factor   1  0.0003356  0.0003356  19.54  0.012
Error    4  0.0000687  0.0000172
Total    5  0.0004043

S = 0.004145   R-Sq = 83.01%   R-Sq(adj) = 78.76%


                          Individual 95% CIs For Mean Based on Pooled StDev
Level  N     Mean    StDev  --------+---------+---------+---------+-
P_AAC  2  0.17001  0.00348  (----------*---------)
C_AAC  4  0.18587  0.00434                      (------*-------)
                          --------+---------+---------+---------+-
                                0.1680    0.1760    0.1840    0.1920

Pooled StDev = 0.00414
```

One-way ANOVA: P_AFRC, C_AFRC

```
Source  DF         SS         MS      F      P
Factor   1  0.0005977  0.0005977  17.92  0.013
Error    4  0.0001334  0.0000333
Total    5  0.0007311

S = 0.005775   R-Sq = 81.76%   R-Sq(adj) = 77.19%


                           Individual 95% CIs For Mean Based on
                           Pooled StDev
Level   N     Mean    StDev  -----+---------+---------+---------+----
P_AFRC  4  0.14654  0.00667  (------*------)
C_AFRC  2  0.16772  0.00032                (---------*---------)
                           -----+---------+---------+---------+----
```

```
                              0.144     0.156     0.168     0.180

Pooled StDev = 0.00577
```

One-way ANOVA: P_FHWA, C_FHWA

```
Source  DF       SS       MS     F      P
Factor   1  0.00131  0.00131  0.38  0.600
Error    2  0.00687  0.00344
Total    3  0.00818

S = 0.05862   R-Sq = 15.98%   R-Sq(adj) = 0.00%

                           Individual 95% CIs For Mean Based on
                           Pooled StDev
Level   N    Mean   StDev  ---------+---------+---------+---------+
P_FHWA  2  1.1208  0.0207     (-----------------*-----------------)
C_FHWA  2  1.0846  0.0803  (-----------------*-----------------)
                           ---------+---------+---------+---------+
                                  1.00      1.10      1.20      1.30

Pooled StDev = 0.0586
```